Synthesis and Reactivity of Anthracene-Based Molecular Precursors for Low-Valent Boron Species

by

Dion S. Sukhram

Submitted to the Department of Chemistry
in partial fulfillment of the requirements for the degree of

Bachelor of Science in Chemistry

at the

MASSACHUSETTS INSTITUTE OF TECHNOLOGY

June 2023

Author .....
Department of Chemistry
May 19, 2023

Certified by .....
Christopher C. Cummins
Henry Dreyfus Professor of Chemistry
Thesis Supervisor

Accepted by .....
Elizabeth M. Nolan
Ivan R. Cottrell Professor of Immunology
Undergraduate Officer, Department of Chemistry

Synthesis and Reactivity of Anthracene-Based Molecular Precursors for Low-Valent Boron Species

by

Dion S. Sukhram

Submitted to the Department of Chemistry
on May 19, 2023, in partial fulfillment of the
requirements for the degree of
Bachelor of Science in Chemistry

Abstract

The study of compounds containing elusive main group multiple bonds has long been a topic of immense interest. Today, it remains an attractive path towards unlocking new reactivity and developing a complete empirical understanding of chemical bonding. However, due in large part to a lack of suitable synthetic methodologies, the chemistry of numerous desirable functionalities remains poorly accessible. Herein, we report the synthesis of the first series of dibenzo-7-boranorbornadienes, or 9,10-bridged boron anthracene (RBA, A = anthracene or $C_{14}H_{10}$) compounds, and their unique properties and reactivity. Oxidation of $^{i}Pr_2NBA$ with an amine oxide was found to lead to the selective formation of the bicyclic borinate ester $^{i}Pr_2NBOA$, an easily isolable solid that unimolecularly fragments to $^{i}Pr_2NBO$ + A upon heating to moderate temperatures in solution. This rare free, monomeric oxoborane has been demonstrated to undergo cycloadditions with a number of organic substrates and efforts to expand both the scope of derivatives and reactivity are underway. The possibility to access species containing highly unstable boron-pnictogen triple bonds has also been explored via the synthesis of the azidoborane trimer $(N_3BA)_3$ and cyclic(alkyl)(amino)carbene (CAAC) stabilized boraphosphaketene ^{Et}CAAC·ABPCO. Preliminary and ongoing reactivity studies are discussed.

Thesis Supervisor: Christopher C. Cummins
Title: Henry Dreyfus Professor of Chemistry

Contents

Chapter 1

The First Well-Characterized Dibenzo-7-boranorbornadienes

1.1 Introduction

The use of benzene, naphthalene, anthracene, and other acenes as platforms for the construction of molecular precursors has proven to be a useful method for the liberation of interesting low-coordinate reactive intermediates; this subject has been discussed in immense detail in the doctoral thesis of former Cummins lab member Prof. Wesley Transue and thus will not be repeated here.[1] Among the known derivatives are 7-boranorbornadienes, which constitute a somewhat well-studied class of compounds.[1–6] The synthetic usefulness of these species in generating low-valent boron fragments has thus far been limited by their thermal instability, rearranging to form borepins, and the reactivity of the carbon-carbon double bond, among other factors. Thus, we initially set out to prepare the anthracene derivatives as potential sources of reactive free borylenes, analogous to the established phosphinidine reactivity of dibenzo-7-phosphanorbornadienes.[7,8] Although the thermodynamic driving force of rearomatization associated with anthracene elimination is expected to be significantly lower than that of benzene, a higher degree of synthetic manipulability is evidently desirable.

Upon examination of the literature, it was found that a single example of a

dibenzo-7-boranorbornadiene, (2,6-^{t}Bu$_2$PhO)BA (A = $C_{14}H_{10}$ or Anthracene) may be found in the Cambridge Structural Database, submitted via a private communication from Nöth and co-workers.[9] Having never been formally published, the properties of this molecule remained unknown. We initially attempted to directly replicate its synthesis via the reaction of MgA(THF)$_3$ and the corresponding aryloxyboron dichloride, but to no avail. Upon further study, it was found that substantial π-stabilization of the dihaloborane is critical to the success of this reaction in forming the desired bridged compound, rather than leading to its reduction to form tetracoordinate borates. Many such compounds are additionally reactive towards ethers, leading to the ring-opening of tetrahydrofuran, and thus entirely incompatible with MgA(THF)$_3$.

1.2 Synthesis and Reactivity of Derivatives

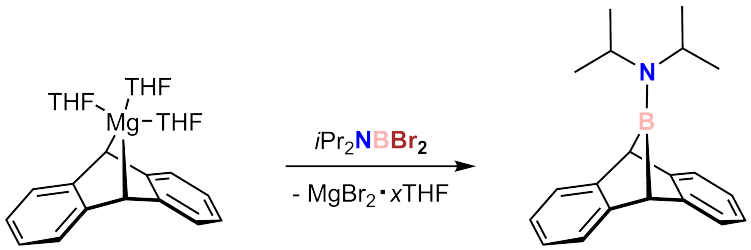

Figure 1-1: Direct synthesis of ^{i}Pr$_2$NBA via salt elimination using MgA(THF)$_3$.

Visiting researcher Anna Ordyszewska turned to the ether-stable borane ^{i}Pr$_2$NBBr$_2$, which reacted at -78 °C with MgA(THF)$_3$ in THF solution to give a mixture of the desired product, ^{i}Pr$_2$NBA, and *trans*-9,10-(^{i}Pr$_2$NBBr)$_2$DHA (DHA = 9,10-dihydroanthracene), identified by their ^{11}B chemical shifts of δ 40.6 and 31.4 ppm, respectively. These two compounds co-crystallized upon storage of the crude solutions at low temperature and were characterized by single crystal x-ray diffraction (Fig. 1-2). In later experimental studies, I found that the bridged compound may be selectively synthesized in yields of up to 90% via slow addition of the dibromoborane to a slurry of MgA(THF)$_3$ in dimethoxyethane at room temperature.

^{i}Pr$_2$NBA was found to have a relatively short B-N bond length of 1.375 Å, which

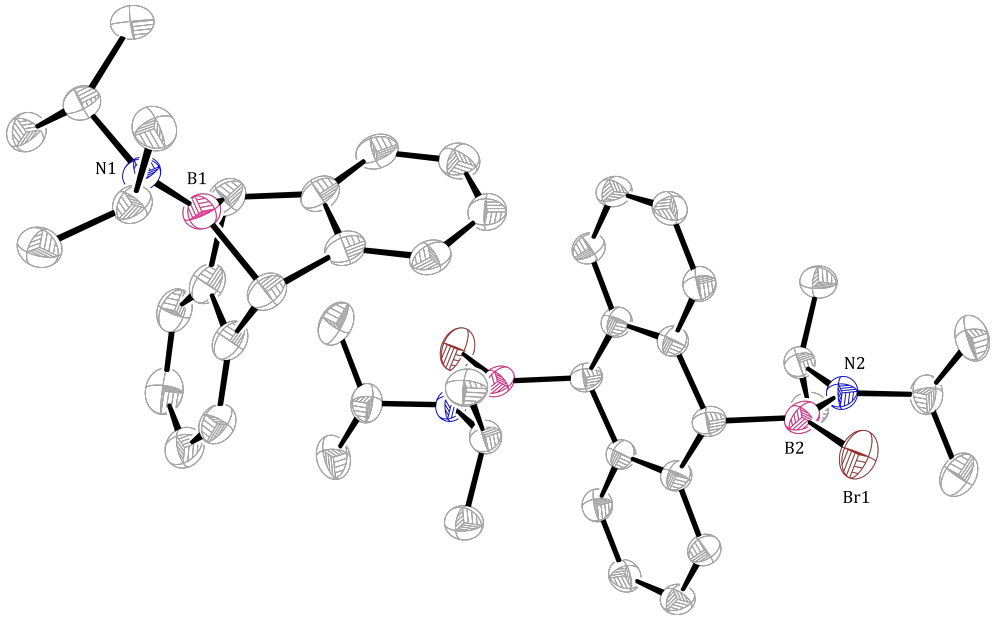

Figure 1-2: Molecular structures of $^{i}Pr_2NBA$ and *trans*-9,10-($^{i}Pr_2NBBr)_2DHA$, shown with ellipsoids at the 50% probability level and hydrogen atoms omitted for clarity.

is equal to the sum of double bond covalent radii and indicative of the level of stabilization provided by lone pair donation from nitrogen to the empty orbital on boron. Given this observation, I first investigated the ability of this compound to release or transfer an aminoborylene. Unfortunately, $^{i}Pr_2NBA$ was found to exhibit strong thermal stability in both the solid and solution states, and likewise showed little to no activity under photolytic conditions using 254 nm light. Several chemical approaches for borylene transfer were tested, such as addition of stoichiometric $(CpFe(CO)_2)_2$ or $(Ph_3P)_2Pt(C_2H_4)$ to $^{i}Pr_2NBA$ solutions, however no reactivity was observed. Addition of a base-stabilized N-heterocyclic silylene to favor release of anthracene and the borylene fragment showed that $^{i}Pr_2NBA$ would not bind even a moderately bulky neutral donor ligand, thus I turned towards transformation of this starting material with hopes of preparing a variety of less stabilized and less sterically hindered RBA molecules.

The chemical reactivity of $^{i}Pr_2NBA$ has proven to be quite unique given its strong B-N double bond, the poor leaving potential of an amino group, and the properties imbued by the anthracene moiety. It was initially thought that alkoxy- and aryloxy-

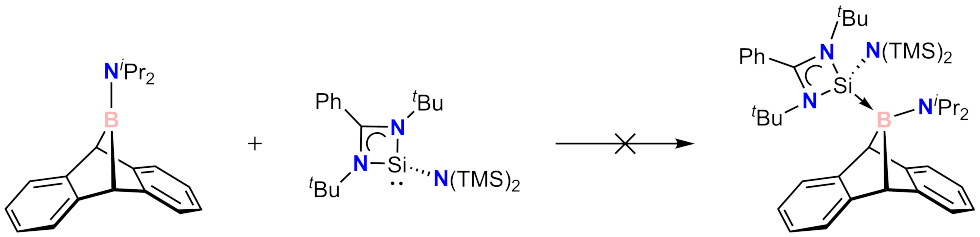

Figure 1-3: ^{i}Pr$_2$NBA does not bind typical strong Lewis bases due to a combination of electronic and steric effects. Neither complexation nor anthracene elimination was observed upon heating to 80 °C.

derivatives could be easily prepared by alcoholysis of the aminoborane, which is indeed a very typical literature procedure,[10] however treatment with small alcohols (methanol, ethanol, isopropanol) instead led to protonation of anthracene to form 9,10-dihydroanthracene and borate esters. Larger alcohols, such as *tert*-butanol or phenol, displayed little to no reactivity at room temperature due to sterics, with slow DHA formation upon heating (Table 1.1).

Alcohol	Observed Result
MeOH	$(MeO)_3B$ + DHA formation
^{i}PrOH	$(^i PrO)_3B$ + DHA formation
^{t}BuOH	No reaction
Propofol	No reaction
PhOH	Slow alcoholysis + DHA formation

Table 1.1: Observed reactivity of ^{i}Pr$_2$NBA towards a representative set of simple alcohols. Methanolysis occurs at room temperature, while other reactions were carried out at 60 to 80 °C in benzene solution. Significant quantities of DHA are observed even with equimolar quantities of borane and alcohol.

This issue was circumvented via addition of stoichiometric ethereal hydrogen chloride to a solution of ^{i}Pr$_2$NBA and an unreactive alcohol, ^{t}BuOH, leading to precipitation of [^{i}Pr$_2$NH$_2$]Cl. As desired, ^{t}BuOBA was found to be easily isolable as a highly crystalline solid that appears to exist as a dimer in solution according to its relatively high field ^{11}B NMR resonance at δ 36.7 ppm and high-symmetry ^{1}H spectrum.

In order to allow for direct nucleophilic substitution at boron, we aimed to synthesize haloborane ClBA and have successfully done so via multiple methods. Treatment of ^{i}Pr$_2$NBA with ethereal HCl lead to the formation of its amine adduct,

$^{i}Pr_2NH{\cdot}ClBA$. The second protonation occurs somewhat slowly, with a large excess of hydrogen chloride solution and several hours of stirring needed to reach completion. $ClBA{\cdot}Et_2O$ may be isolated as a colorless powder that is poorly soluble in ether, hydrocarbons, and arenes, but soluble in dichloromethane and THF. Separation and purification from the quaternary ammonium salt is thus made relatively difficult and requires undesirably large quantities of diethyl ether and multiple recrystallizations. One option that was found is its isolation as a THF adduct, due to its higher solubility, however the presence of tetrahydrofuran is undesirable in some cases given its greater potential for unwanted reactivity towards the products of later substitution reactions. Moreover, the solvent donor was not found to be easily removable. An alternative route making use of ^{t}BuOBA and PCl_5 as the chloride source was developed, allowing for the easier isolation of $ClBA{\cdot}Et_2O$ via its precipitation from ether solution. Lewis base-free ClBA is hypothesized to not be sufficiently stable for isolation, and attempts at this reaction in pentane or dichloromethane lead to the formation of free anthracene, PCl_3, $[PCl_4]^+$, and numerous boron species according to ^{1}H, ^{31}P, and ^{11}B NMR spectroscopy. Isolation of the free triflate ABOTf via treatment of $^{i}Pr_2NBA$ with triflic acid was also explored, but to no avail.

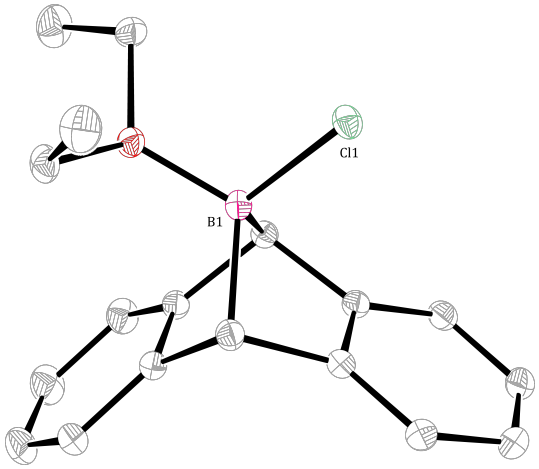

Figure 1-4: Molecular structure of $ClBA{\cdot}Et_2O$, shown with ellipsoids at the 50% probability level and hydrogen atoms omitted for clarity.

Given the lack of lone pair electron density on nitrogen, other potential routes for substitution from $^{i}Pr_2NBA$ that are described for aminoboranes in the litera-

ture were found to be surprisingly unproductive. For instance, no coordination to or ligand redistribution with strongly Lewis acidic BX_3 (X = Cl, Br) or $BF_3{\cdot}Et_2O$ could be observed. Moreover, no reactivity towards very strong alklyating agents such as MeOTf or Meerwein's salt, $[R_3O][BF_4]$ (R = Me, Et), is observed at room temperature, however heating such a mixture leads to formation of multiple products including $BF_3{\cdot}Et_2O$ in the latter case, which is proposed to occur via generation of a reactive borenium and subsequent fluoride abstraction from the non-innocent tetrafluoroborate counteranion.

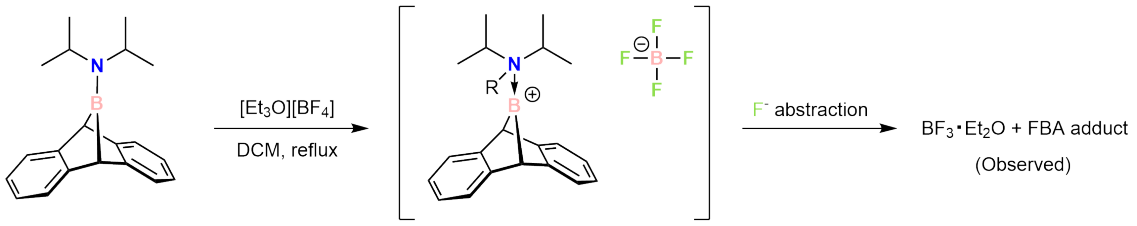

Figure 1-5: Inferred generation of an unstable anthracene-based borenium via alkylation under reflux conditions. Only a very small quantity of FBA, as either an amine or ether adduct, may be observed in solution, presumably due to its poor thermal stability.

Inspired by this result, it has been proposed that silylation at nitrogen with an isolable silylium species such as $[Et_3Si{\cdot}Toluene][BArF_{20}]$ may offer a halide-free route towards nucleophilic substitution at boron, however this option has not yet been properly investigated due to difficulties with handling such reactive reagents under typical glovebox conditions and greater costs associated with the use of such reagents making it less attractive.

Interestingly, $^{i}Pr_2NBA$ was found to react slowly with borane dimethylsulfide in pentane solution, leading to precipitation of $HBA{\cdot}SMe_2$. It is not entirely clear why this transformation occurs readily whereas those with other BX_3 do not, however this might be attributed to the greater stability of XBA in the presence of an unreactive donor such as dimethylsulfide. Reactions with other commercially available $BX_3{\cdot}SMe_2$ have not yet been tested, however they may offer yet another route for further substitution. The case of $BBr_3{\cdot}SMe_2$ is especially interesting, as it would presumably lead to precipitation of $BrBA{\cdot}SMe_2$ with formation of $^{i}Pr_2NBBr_2$ in solution,

which may be isolated and recycled for the synthesis of more starting material.

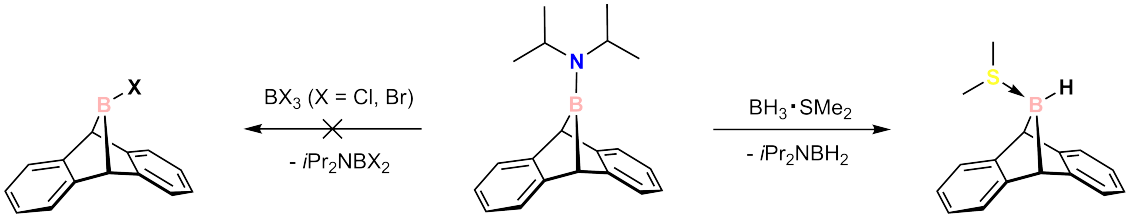

Figure 1-6: Observed reactivity of $^{i}Pr_2NBA$ towards simple electrophilic boranes.

Numerous other methods for the synthesis of HBA and its adducts were initially attempted, mainly via ClBA·Et_2O, but with very limited success. Treatment with equimolar $NaBH_4$ in THF solution led to formation of HBA·THF as confirmed by multinuclear NMR, however this reaction takes many days to go to completion and leads to the formation of a substantial quantity of BH_3·THF, which might be undesirable at larger scales. Routes using $LiAlH_4$, as is frequently relied upon in the relevant literature, were explored: addition of the hydride in minimal stoichiometry led to the formation of HBA·THF with loss of $LiAlCl_4$, whereas the use of two equivalents of LAH led to the selective formation of the borohydride LiH_2BA, which is easily observed as a relatively sharp triplet centered at δ 5.01 ppm in the ^{11}B NMR spectrum. Subsequent treatment of this compound with chlorotrimethylsilane led to elimination of TMS-H and LiCl to form HBA·THF, observed as a singlet at ^{11}B δ 15.6 ppm that is broadened by unresolved B-H coupling.

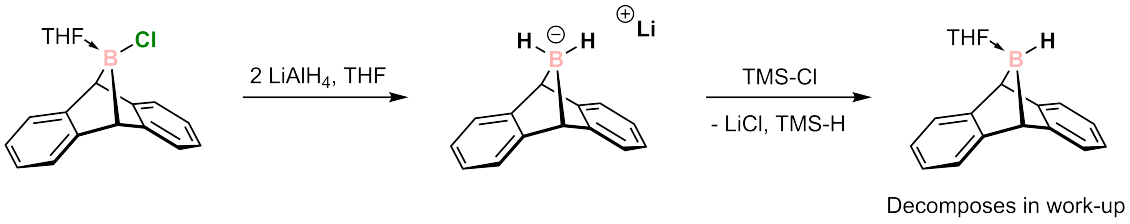

Figure 1-7: Synthesis of LiH_2BA and its treatment with TMSCl for the initial preparation of HBA·THF *in situ*. The product could not be isolated and is presumed to be reactive towards residual dissolved aluminum species and/or the solvent.

Unfortunately, in each of these cases the product could only be observed in solution and concentration under vacuum led to the formation of unassignable broad signals

in the ^{11}B and ^{1}H spectra and/or the formation of insoluble materials in all cases. It is hypothesized that the target compound is very fragile and prone to reaction with the salts formed as byproducts in its synthesis and/or the etheral solvents present in these cases.

In order to explore ether-free routes towards the isolation of electrophilic RBA compounds such as HBA and MeBA, I investigated the reactivity of my starting materials towards common aluminum reagents. Upon treatment of ^{i}Pr$_2$NBA with a slight stochiometric excess of diisobutylaluminum hydride, near-complete conversion was observed to a new poorly soluble species exhibiting a broad ^{11}B resonance at δ 33.2 ppm. Although initially assigned as the desired hydroborane dimer (HBA)$_2$, proton NMR revealed the presence of multiple signals in the alkyl region, including those characteristic of the isopropyl groups. Separation of the solid components was attempted via sublimation, however the material collected on the cold finger was identified as ^{i}Pr$_2$NBA and free anthracene. It was thus inferred that, rather than fully transferring a hydride, a borane-alane adduct was formed. Analagous reactivity was observed with the smaller trimethylaluminum: addition of stoichiometric AlMe$_3$ to a solution of ^{i}Pr$_2$NBA gives rise to a new species that shows up as a moderately sharp singlet at δ 45.4 ppm in the ^{11}B NMR spectrum, corresponding to the adduct.

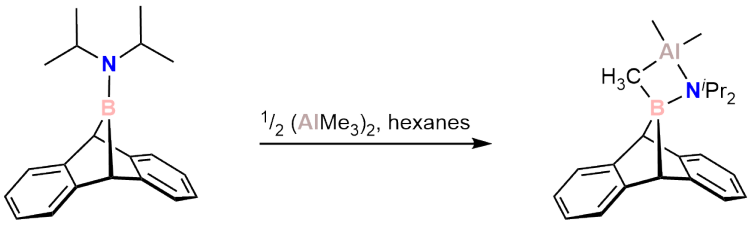

Figure 1-8: Observed reactivity of ^{i}Pr$_2$NBA towards trimethylaluminum in hexane solution. Methyl exchange does not occur readily, and an alumane-borane adduct is instead obtained.

Curious about the nature of the bonding in this compound, and whether it is best described as an adduct of ^{i}Pr$_2$NBA or of MeBA, [^{i}Pr$_2$NBA][AlMe$_3$] or [MeBA][^{i}Pr$_2$NAlMe$_2$], its geometry was optimized *in silico* and found to indeed have bond lengths consistent with a stronger covalent Al-N interaction (calculated length shorter than the sum of covalent radii), with a moderately strong dative interaction

between the nitrogen lone pair and boron empty orbital (see Section 1.5.1). It is thus expected that addition of a relatively strong Lewis base would displace the alane to form the complex LB·MeBA and $(^{i}Pr_2NAlMe_2)_2$, however this has not been directly tested due to desirability of the free borane. Moreover, this reaction is not especially clean, with the reaction mixture turning orange in color and over-reaction to form a noticeable quantity of BMe_3 being confirmed by NMR. Analogous treatment of ^{t}BuOBA with $AlMe_3$ appears to be a better potential option according to preliminary results, given the weaker donor properties of oxygen, however studies on this reaction and its optimization are still in progress. Finally, the treatment of ClBA·Et_2O with $AlCl_3$ was initially of interest as a route to anthracene-based diboron compounds, but this reaction is thought to be severely complicated by the presence of a Lewis base. Combination of reagents in stoichiometric quantities resulted in a translucent brown solution and loss of ^{11}B signal. Addition of two molar equivalents of $AlCl_3$ to a solution of ClBA·Et_2O in DCM resulted in dramatic darkening of the solution and NMR revealed two moderately sharp ^{11}B resonances at δ 46.5 and 26.3 ppm, a single ^{27}Al signal at 101.4 ppm, and extremely broadened aryl ^{1}H signals, but the identity of the product(s) has not yet been determined.

1.3 Experimental Details

1.3.1 General Information

Except as otherwise noted, all manipulations were performed in a Vacuum Atmospheres model MO-40M glovebox under an inert atmosphere of purified N_2. All solvents were obtained anhydrous and oxygen-free by bubble degassing (Ar), passage through columns of alumina using a solvent purification system (Pure Process Technology, Nashua, NH),[11] and storage over 4.0 Å molecular sieves.[12] Deuterated solvents were purchased from Cambridge Isotope Labs and degassed by three freeze-pump-thaw cycles and stored over 4 Å molecular sieves for at least 48 h prior to use. Diatomaceous earth (EM Science) and 4 Å molecular sieves were dried by heating

above 200 °C under dynamic vacuum for at least 48 h prior to use. All glassware was dried in an oven for at least two hours at temperatures greater than 150 °C.

$MgA(THF)_3$[8] and $^iPr_2NBBr_2$[13] were prepared according to literature procedures. ^{t}BuOH (Sigma-Aldrich) was degassed and stored over 4.0 Å molecular sieves prior to use. $LiAlH_4$ (Alfa-Aesar) was purified from diethyl ether solution.[14] $[Et_3O][BF_4]$ (Alfa-Aesar), trimethylaluminum solution (Sigma-Aldrich), ethereal hydrogen chloride solution (Sigma-Aldrich), phosphorus pentachloride (Sigma-Aldrich), aluminum trichloride (Alfa-Aesar), and borane dimethylsulfide complex (Sigma-Aldrich) were used as received.

NMR spectra were obtained on a Bruker Avance 400 instrument equipped with a Magnex Scientific or with a SpectroSpin superconducting magnet or on a Bruker Avance 500 instrument equipped with a Magnex Scientific or with a SpectroSpin superconducting magnet. ^{1}H and ^{13}C NMR spectra were referenced internally to residual solvent signals.[15] ^{11}B NMR spectra were externally referenced to 15% $BF_3{\cdot}Et_2O$ in $CDCl_3$ (0 ppm).

High resolution mass spectral (HRMS) data were collected using a Jeol AccuTOF 4G LC-Plus mass spectrometer equipped with an Ion-Sense DART source. Data were calibrated to a sample of PEG-600 and were collected in positive-ion mode. Samples were prepared in pentane or dichloromethane (ca. 10 μM concentration) and were briefly exposed to air before being placed in front of the DART source.

1.3.2 Synthesis of ^{i}Pr$_2$NBA

To a stirring slurry of $MgA(THF)_3$ (7.73 g, 18.5 mmol, 1.0 equiv) in dimethoxyethane (200mL) was added a solution of $^iPr_2NBBr_2$ (5.00 g, 18.5 mmol, 1.0 equiv) in dimethoxyethane (20 mL) dropwise at room temperature. After complete addition of the dibromoborane, the reaction mixture was stirred for an hour then volatiles were removed from the resulting dull yellow suspension under reduced pressure. The residues were resuspended in diethyl ether (200 mL) and filtered through a one inch plug of charcoal and celite. The solvent was removed in vacuo and the slightly yellow solids were transferred to a 20 mL scintillation vial. Pentane (5 mL)

was added and the vial agitated to wash the solids, before being stored in a -35 °C freezer overnight. The supernatant was removed via pipet and the solids dried under vacuum, yielding $^{i}Pr_2NBA$ as an off white powder (4.69 g, 16.2 mmol, 88%). ^{1}H NMR (500 MHz, C_6D_6, 25 °C) δ 7.34 (dd, J = 5.3, 3.1 Hz, 4H), 7.04 (dd, J = 5.3, 3.2 Hz, 4H), 3.78 (s, 2H), 3.10 (hept, J = 6.8 Hz, 2H), 0.80 (d, J = 6.8 Hz, 12H) ppm. ^{11}B NMR (128 MHz, chloroform-d, 25 °C) δ 40.45 ppm. $^{13}C\{^{1}H\}$ NMR (101 MHz, chloroform-d, 25 °C) δ 146.40, 124.74, 121.66, 47.27, 44.89, 23.23 ppm.

Mass spectrum of $^{i}Pr_2NBA$

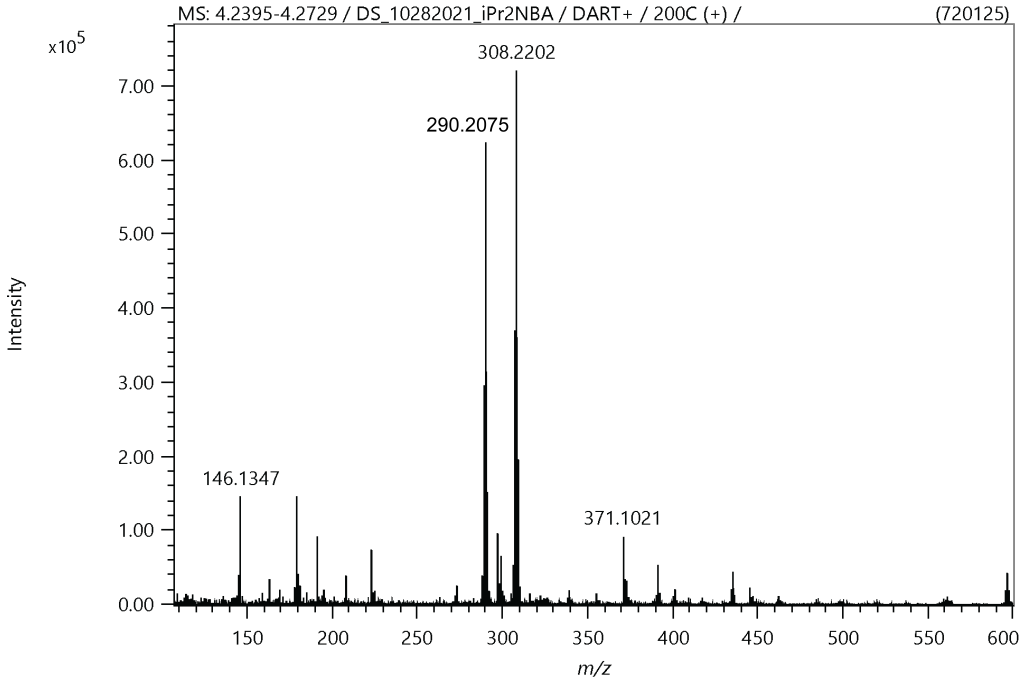

Figure 1-9: DART-HRMS analysis of $^{i}Pr_2NBA$ collected with an open-air source at 200 °C. The [M+H] peak is observed at m/z = 290.2075 (calc. 290.2102). Due to the presence of moisture, a large signal at m/z = 308.2202 corresponding to $[M+H+H_2O]$, or $^{i}Pr_2NH{\cdot}HOBA$ (calc. 308.2186), is also observed.

Thermal stability of $^{i}Pr_2NBA$

A sample of $^{i}Pr_2NBA$ was transferred to a glass capillary and flame-sealed. Using this sample, the material was found to melt at 114 to 117 °C. The capillary was returned

to the glovebox, crushed in a vial, and the residues dissolved in deuterated benzene. ^{1}H NMR revealed that the compound remained fully intact through heating to this temperature in the solid state.

A sample of ^{i}Pr$_2$NBA (approximately 10 mg) were transferred to a J Young tube and dissolved in 0.7 mL mesitylene. The tube was sealed and placed in a 150 °C oil bath in the fume hood for several hours. ^{1}H NMR indicated that the compound remained intact upon heating to this temperature in solution (Fig. 1-10).

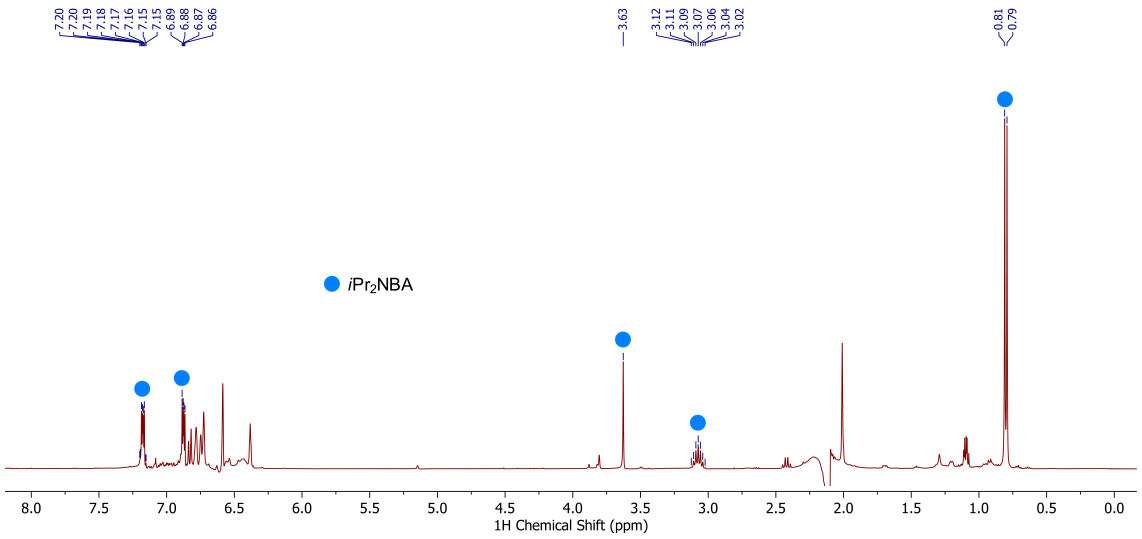

Figure 1-10: ^{1}H NMR (400 MHz, solvent-suppressed, protonated mesitylene) of ^{i}Pr$_2$NBA after heating to 150 °C. No signal corresponding to free anthracene were observed. Additional aryl signals and singlet in the aliphatic region are attributed to toluene present as a contaminant.

Treatment of ^{i}Pr$_2$NBA with [Et$_3$O][BF$_4$]

^{i}Pr$_2$NBA (120 mg, 0.415 mmol, 1 equiv) was weighed out in a 25 mL Schlenk flask and dissolved in dichloromethane (10 mL). Solid [Et$_3$O][BF$_4$] (80 mg, 0.421 mmol, 1.01 equiv) was added and dissolved with stirring. The reaction vessel was removed from the glovebox and set up under nitrogen pressure for reflux in the fumehood. After heating for 16 hours, the flask was cooled, capped with a stopper, and returned to the glovebox. An aliquot of the crude mixture was transferred to an NMR tube for analysis. ^{11}B NMR revealed that the starting material remained mostly unconverted,

however a new small doublet at δ 17.19 ($^1J_{BF}$ = 84.3 Hz) could be identified, along with the presence of $BF_3{\cdot}Et_2O$ (Fig. 1-11). It was inferred that slow conversion to thermally unstable FBA as either an ether or amine adduct occurs under these conditions. A corresponding ^{19}F resonance could not be identified due to the low concentration and broadening by adjacent boron, but the presence of a small amount of free anthracene was separately confirmed by ^1H NMR.

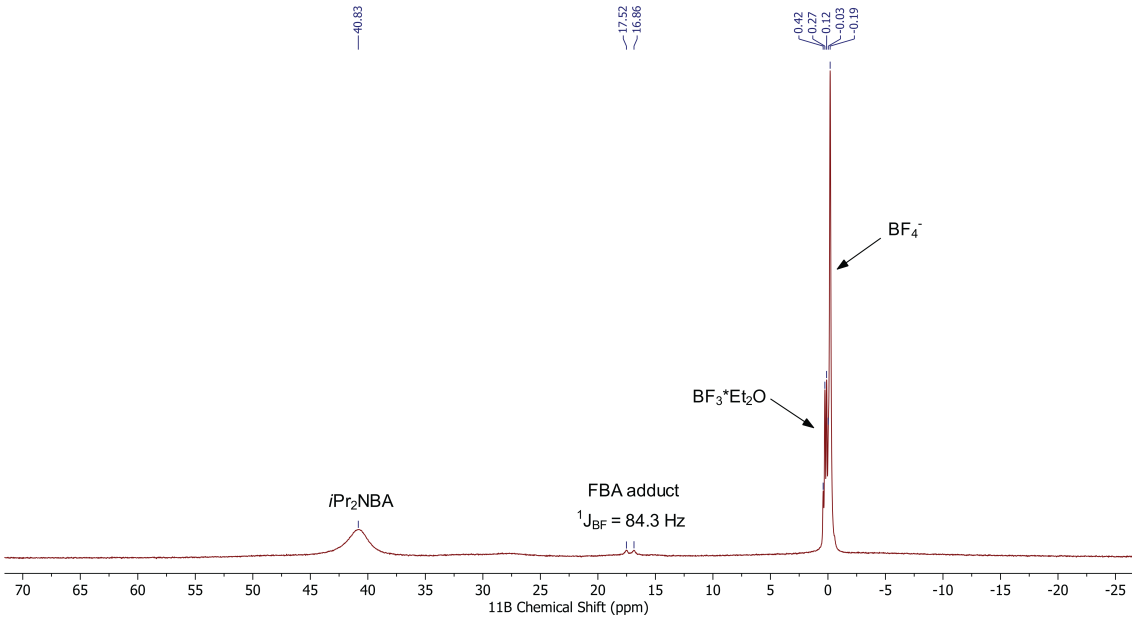

Figure 1-11: ^{11}B NMR (128 MHz, CH_2Cl_2, 25 °C) of a solution of $^iPr_2NBA$ after treatment with $[Et_3O][BF_4]$ in refluxing dichloromethane overnight.

Treatment of $^iPr_2NBA$ with $(AlMe_3)_2$

To a solution of $^iPr_2NBA$ (116 mg, 0.401 mmol, 1 equiv) in hexanes (8 mL) was added trimethylaluminum (0.2 mL of a 2.0 M hexane solution) dropwise via syringe at ambient temperature. The vial was capped and the reaction mixture stirred for 16 hours. The resulting heterogenous mixture was filtered through glass microfiber filter paper and the orange filtrate collected, then an aliquot transferred to an NMR tube for analysis. A new and relatively sharp ($\nu_{1/2}$ = 66.2 Hz) ^{11}B resonance was observed at δ 45.4 ppm, corresponding to the adduct (Fig. 1-12). The solids formed were separately analyzed and were found to consist primarily of free anthracene formed by

some amount of over-methylation with evolution of BMe_3.

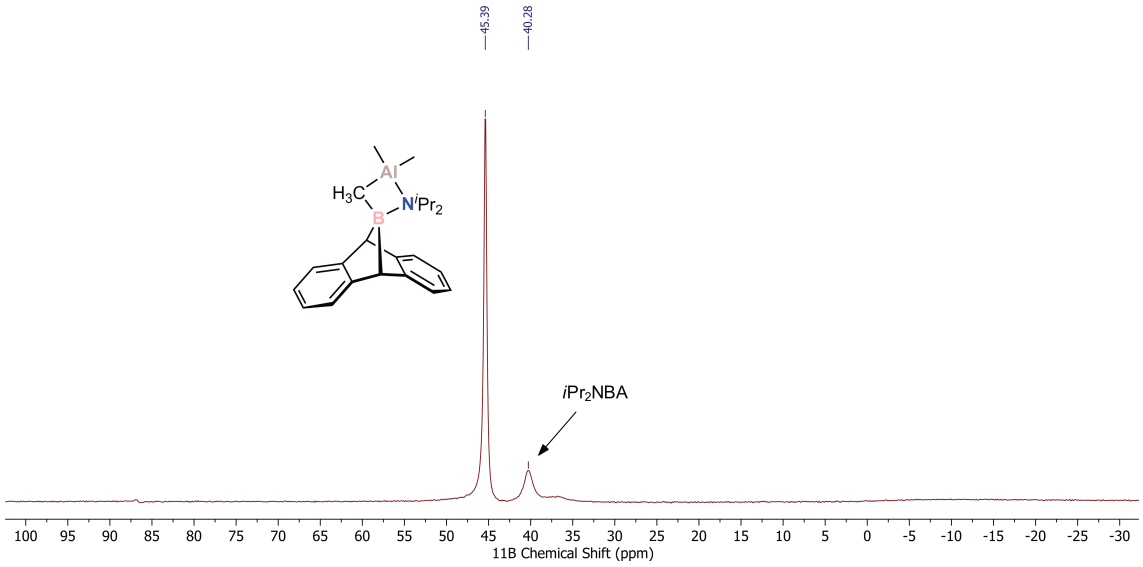

Figure 1-12: Observed reactivity of $^{i}Pr_2NBA$ towards trimethylaluminum in hexane solution by ^{11}B NMR (160 MHz, Hexanes, 25 °C). Methyl exchange does not occur readily, and an alumane-borane adduct is instead obtained.

1.3.3 Synthesis of ^{t}BuOBA

To a solution of $^{i}Pr_2NBA$ (3.00 g, 10.4 mmol, 1.0 equiv) in Et_2O (50mL) was added ^{t}BuOH (768 mg, 10.4 mmol, 1.0 equiv). The reaction flask was capped with a SubaSeal septum and placed under 1 atm of nitrogen on the Schlenk line. 1.0 M ethereal HCl solution (10.5 mL, 1.01 equiv) was added dropwise to the stirring solution via syringe, resulting in the development of a colorless precipitate. After two hours, volatiles were removed under reduced pressure and the flask returned to the glovebox. The residues were resuspended in pentane (100 mL) and filtered through a medium sintered frit with a 1 inch plug of celite and activated charcoal. The flask and filter were rinsed thrice with more pentane (300 mL total) then solvent removed from the combined colorless filtrates *in vacuo*. ^{t}BuOBA was obtained as a voluminous colorless solid (2.313 g, 8.83 mmol, 85%. ^{1}H NMR (400 MHz, Benzene-d_6, 25 °C) δ 7.29 (dd, J = 5.4, 3.2 Hz, 4H), 7.04 (dd, J = 5.4, 3.2 Hz, 4H), 3.80 (s, 2H), 0.93 (s, 9H) ppm. ^{11}B NMR (128 MHz, Benzene-d_6, 25 °C) δ 36.67 ppm. $^{13}C\{^{1}H\}$ NMR (101

MHz, Benzene-d_6, 25 °C) δ 144.21, 125.92, 122.63, 76.96, 44.95, 29.81 ppm.

1.3.4 Synthesis of ClBA·^{i}Pr$_2$NH

^{i}Pr$_2$NBA (50 mg, 0.173 mmol, 1.0 equiv) was dissolved in diethyl ether (6 mL) in a small Schlenk flask. The reaction vessel was sealed, removed from the glovebox, placed under nitrogen pressure on the Schlenk line, and cooled to -78 °C in a dry ice/acetone bath. Ethereal HCl (0.18 mL of a 2.0 M solution, 2.1 equiv) was added dropwise via syringe, turning the mixture cloudy. The flask was removed from the cold bath and allowed to warm to room temperature with stirring, then volatiles were removed under reduced pressure. The flask was returned to the glovebox and a sample of the material taken for NMR, revealing it to be ClBA·^{i}Pr$_2$NH with a small amount of unreacted ^{i}Pr$_2$NBA. Although its identity has been confirmed by multinuclear NMR, this compound has not been isolated in a pure form due to greater preference of a non-protic, more labile Lewis base for use in later reactions. ^{1}H NMR (400 MHz, Benzene-d_6, 25 °C) δ 7.47 to 6.88 (m, 8H), 3.54 (s, 2H), 3.06 (m, 1H), 2.73 (br s, 1H), 2.57 (hept, 1H), 0.75 (d, 6H), 0.69 (d, 6H) ppm. ^{11}B NMR (128 MHz, Benzene-d_6, 25 °C) δ 15.38 ppm.

1.3.5 Synthesis of ClBA·Et$_2$O

Via ^{i}Pr$_2$NBA, developed in part by André K. Eckhardt

In the glovebox, a 250 mL Schlenk flask was charged with a solution of ^{i}Pr$_2$NBA (500 mg, 1.73 mmol, 1 equiv) in diethyl ether (150 mL). The vessel was capped with a rubber septum, transferred to the fumehood, and placed under nitrogen pressure on the Schlenk line. Hydrogen chloride solution (1.0 M in Et$_2$O, 17.3 ml, 10 equiv) was added to the solution via syringe with rapid stirring. A white precipitate immediately developed. After the addition, the mixture was stirred for two hours at room temperature, then the flask placed under reduced pressure to degas the solution. The punctured septum was sealed with grease and electrical tape then, under vacuum, the reaction flask was returned to the glovebox. The mixture was

filtered through a one inch plug of celite and charcoal in a medium frit. The plug was washed with an additional 150 mL diethyl ether. The combined filtrates were collected and evaporated under reduced pressure, yielding ClBA·Et_2O as a colorless powder (360 mg, 69.7 %). ^{1}H NMR (Benzene-d6, 400 MHz, 25 °C) δ 7.29 (m, 4H), 7.00 (m, 4H), 3.47 (s, 2H), 3.36 (q, 4H, J = 7.2 Hz), 0.51 (t, 6H, J = 7.2 Hz) ppm. ^{13}C{^{1}H} NMR (Benzene-d6, 101 MHz, 25 °C) δ 149.7, 124.5, 122.7, 72.0 (Et_2O), 50.0 (b, bridgehead C, $\nu_{1/2}$ 116.4 Hz), 13.2 (Et_2O) ppm. ^{11}B NMR (Benzene-d6, 128 MHz, 25 °C) δ 19.8 ppm.

Via ^{t}BuOBA

^{t}BuOBA (262 mg, 1.00 mmol, 1.00 equiv) was weighed out in a Schlenk flask and dissolved in Et_2O (10mL). With vigorous stirring, solid PCl_5 (208 mg, 1.00 mmol, 1.00 equiv) was added to the solution portionwise over five minutes. Within several minutes, a colorless precipitate began to develop and the heterogenous reaction mixture was stirred at ambient temperature for approximately two hours. The mixture was loaded into a pipette filter containing a piece of glass microfiber filter paper and the solids collected. The flask and filter were washed thrice with ether (6 mL). Dichloromethane (5 mL) was added to dissolve the solids, and the resulting solution passed through the filter into a clean vial. Solvent was removed *in vacuo*, leaving solid and nearly pure ClBA·Et_2O that could be further purified by recrystallization.

Treatment of ClBA·Et_2O with $AlCl_3$

To a solution of ClBA·Et_2O (10 mg, 0.034 mmol, 1.0 equiv) in DCM (1.5 mL) was added solid $AlCl_3$ (9.4 mg, 0.070 mmol, 2.1 equiv) with rapid stirring. The reaction mixture became very dark with some precipitate formation. After one hour, an aliquot was transferred to an NMR tube. ^{11}B NMR analysis indicated complete consumption of ClBA·Et_2O, with two new relatively sharp resonances at δ 46.5 and 26.3 ppm being detected (Fig. 1-13); it is unclear if these signals are correlated or entirely distinct. The proton spectrum was severely broadened and did not provide any additional

information.

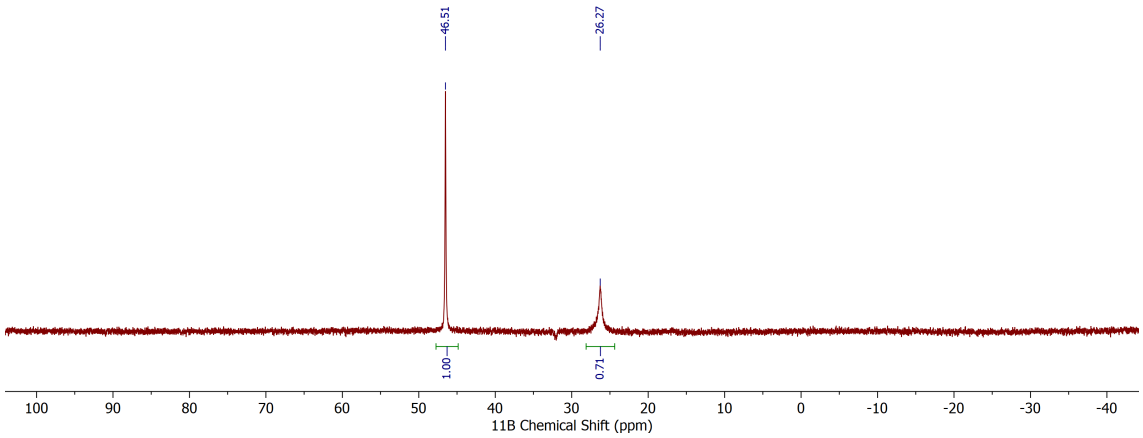

Figure 1-13: ^{11}B NMR (128 MHz, CH_2Cl_2, 25 °C) spectrum of a solution of ClBA·Et_2O after treatment with two equivalents of $AlCl_3$.

1.3.6 Synthesis of ClBA·THF

ClBA·THF was prepared similarly to the diethyl ether adduct from $^{i}Pr_2NBA$: In the glovebox, a 250 mL Schlenk flask was charged with a solution of $^{i}Pr_2NBA$ (3.0 g, 10.4 mmol, 1 equiv) in diethyl ether (150 mL). The vessel was capped with a rubber septum, transferred to the fumehood, and placed under nitrogen pressure on the Schlenk line. Hydrogen chloride solution (2.0 M in Et_2O, 51.9 ml, 10 equiv) was added to the solution via syringe with rapid stirring. A white precipitate immediately developed. After the addition, the mixture was stirred for two hours at room temperature, then all volatiles were removed under reduced pressure. The flask was returned to the glovebox, where the residues were resuspended in THF (50 mL) and filtered through a one inch plug of celite and charcoal. The flask and filter were washed with additional THF (30 mL), then the filtrate evaporated to obtain ClBA·THF (2.1 g, 68.4%) as a colorless powder. ^{11}B NMR (160 MHz, CH_2Cl_2, 25 °C) δ 18.0 ppm. A quality ^{1}H NMR spectrum could not be obtained since the peaks appear broadened.

1.3.7 Synthesis of HBA·THF

Via LiH_2BA

To a solution of ClBA·THF (100 mg, 0.338 mmol, 1.0 equiv) in THF (10 ml) was added solid pre-purified $LiAlH_4$ (27 mg, 0.710 mmol, 2.1 equiv). The solution was stirred at room temperature for an hour, then the resulting heterogenous gray mixture filtered through glass microfiber filter paper into a clean vial. NMR analysis of an aliquot of the crude solution indicated complete conversion to borohydride LiH_2BA. ^{11}B NMR (160 MHz, THF-H, 25 °C) δ 5.01 (t, $^1J_{BH}$ = 86.6 Hz) ppm. ^{1}H NMR (500 MHz, THF-H (solvent-suppressed), 25 °C) δ 7.22 (dd, J = 5.1, 3.1 Hz, 4H), 6.84 (dd, J = 5.1, 3.1 Hz, 4H), 3.44 (s, 2H) ppm.

To a THF solution (10 mL) of LiH_2BA as prepared above was added chlorotrimethylsilane (97 mg, 0.890 mmol, 2.6 equiv) via pipette. The solution was stirred at room temperature for 24 hours, during which time it became cloudy. The mixture was filtered through glass microfiber filter paper into a clean vial and an aliquot transferred to an NMR tube for analysis, revealing nearly complete conversion to HBA·THF. ^{11}B NMR (160 MHz, THF-H, 25 °C) δ 15.6 (br s, $\nu_{1/2}$ = 320.3 Hz). ^{1}H NMR (500 MHz, THF-H (solvent-suppressed), 25 °C) δ 7.05 (dd, J = 5.2, 3.2 Hz, 4H), 6.73 (dd, J = 5.3, 3.1 Hz, 4H), 3.38 (q, J = 7.0 Hz, 4H), 3.28 (s, 2H), 1.11 (t, J = 7.0 Hz, 4H) ppm. The compound could be easily observed in solution, but could not be isolated as a pure solid.

Directly via $LiAlH_4$

To a solution of ClBA·Et_2O (84 mg, 0.282 mmol, 4.0 equiv) in THF (10 mL) was added a solution of $LiAlH_4$ in THF (1.0 mL of a 3 mg/mL solution, 1.12 equiv) via syringe. The mixture was stirred at room temperature for six hours, then filtered through glass microfiber filter paper into a clean vial. ^{11}B and ^{1}H NMR analysis indicated nearly complete conversion to HBA·THF, which could not be isolated as a solid.

1.3.8 Synthesis of HBA·SMe_2

To a concentrated solution of $^{i}Pr_2NBA$ (289mg, 1.00 mmol, 1.0 equiv) in pentane (4 mL) was added 10 M BH_3·SMe_2 in excess dimethyl sulfide (0.1 mL, 1.00 mmol, 1 equiv) via syringe. The vial was capped, sealed with electrical tape, and stirred at ambient temperature in the glovebox for 72 hours, with a colorless precipitate developing over time. The heterogeneous mixture was loaded into a pipette filter containing a piece of glass microfiber filter paper and the solids collected. The vial and filter were washed with pentane (5 x 1 mL), then the product was transferred to a tared vial and brought to constant mass under reduced pressure. HBA·SMe_2 of moderate purity (142 mg, 56%) was obtained as a colorless free-flowing powder; the impurities observed by NMR were found to be present in the commercial reagent used and efforts to purify either the starting material or product are ongoing. ^{11}B NMR (160 MHz, CH_2Cl_2, 25 °C) δ 10.52 (d, $^{1}J_{BH}$ = 127.9 Hz) ppm.

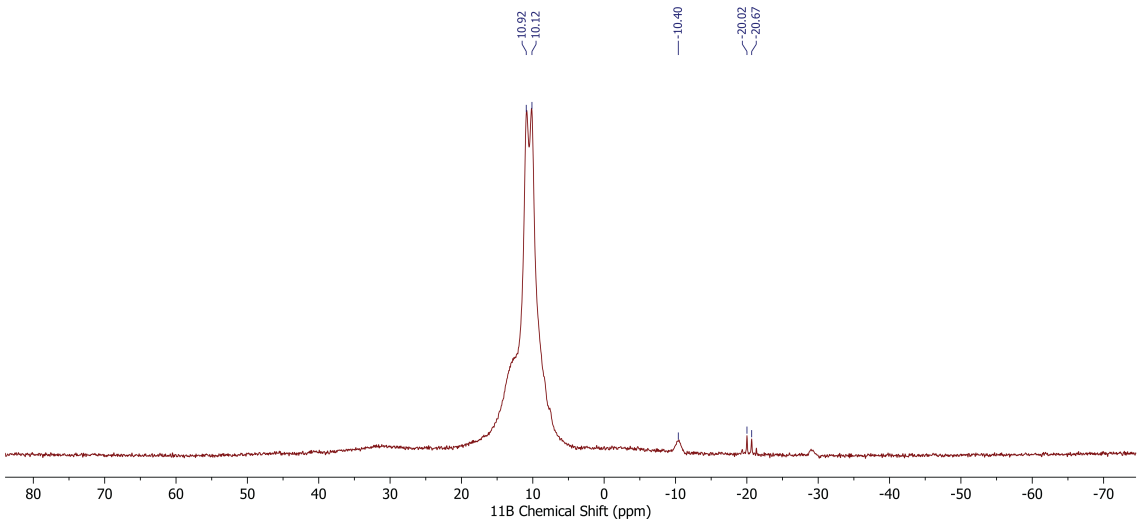

Figure 1-14: ^{11}B NMR (160 MHz, CH_2Cl_2) of crude isolated HBA·SMe_2. The broad signal causing the product resonance to appear asymmetric is thought to be HBA·Et_2O or a similar adduct, formed from ether impurities in the commercial solution.

1.4 X-Ray Diffraction Studies

(Carried out by Anna Ordyszewska and Martin L. Y. Riu)

Single crystals suitable for X-ray diffraction were transferred from the glovebox under Paratone oil onto a microscope slide. A crystal was selected under a microscope and mounted in hydrocarbon oil on a nylon loop. Low-temperature diffraction data were collected on a Bruker-AXS X8 Kappa Duo diffractometer with $I\mu S$ micro-sources, coupled to a Photon 3 CPAD detector using Cu K_α radiation (λ = 1.54178 Å) and a Smart APEX2 CCD detector using Mo K_α radiation (λ = 0.71073 Å), performing ϕ- and ω-scans. The structures were solved by dual-space methods using SHELXT[16] and refined against F^2 on all data by full-matrix least squares with SHELXL-2017[16] following established refinement strategies.[17,18] All non-hydrogen atoms were refined anisotropically. All hydrogen atoms were included into the model at geometrically calculated positions and refined using a riding model. The isotropic displacement parameters of all hydrogen atoms were fixed to 1.2 times the U-value of the atoms they are linked to (1.5 times for methyl groups). Details of the data quality and a summary of the residual values of the refinement are listed in the tables below.

Single co-crystals of ^{i}Pr$_2$NBA and *trans*-9,10-(^{i}Pr$_2$NBBr)$_2$DHA were grown from pentane solution at -35 °C. The structure was solved in the triclinic space group $P\bar{1}$ with one molecule of ^{i}Pr$_2$NBA and half a molecule of *trans*-9,10-(^{i}Pr$_2$NBBr)$_2$DHA in the asymmetric unit; the other half of the latter is generated by an inversion center.

Table 1.2: Crystallographic Data for $^{i}Pr_2NBA$ and *trans*-9,10-($^{i}Pr_2NBBr)_2DHA$

Identification code	P8_200270
Empirical formula, FW (g/mol)	$C_{66}H_{86}B_4Br_2N_4$, 1138.44
Color / Morphology	Colorless / Plate
Crystal size (mm^3)	$0.100 \times 0.100 \times 0.010$
Temperature (K)	100(0)
Wavelength (Å)	1.54178
Crystal system, Space group	Triclinic, $P\bar{1}$
Unit cell dimensions (Å, °)	$a = 7.9586(3)$, $\alpha = 83.290(2)$
	$b = 13.9638(4)$, $\beta = 85.890(2)$
	$c = 13.9761(4)$, $\gamma = 78.053(2)$
Volume ($Å^3$)	1507.34(8)
Z	1
Density (calc., g/cm^3)	1.254
Absorption coefficient (mm^{-1})	2.020
$F(000)$	600
Theta range for data collection (°)	3.188 to 70.210
Index ranges	$-9 \leq h \leq 9$, $-17 \leq k \leq 17$,
	$-17 \leq l \leq 16$
Reflections collected	46380
Independent reflections, R_{int}	5724, 0.0823
Completeness to $\theta_{\max}$ (%)	100.0
Absorption correction	Psi-scan
Refinement method	Full-matrix least-squares on F^2
Data / Restraints / Parameters	5724 / 0 / 351
Goodness-of-fit[a]	1.080
Final R indices[b] $[I > 2\sigma(I)]$	$R_1 = 0.0528$, $wR_2 = 0.1422$
R indices[b] (all data)	$R_1 = 0.0654$, $wR_2 = 0.1514$
Largest diff. peak and hole ($e \cdot Å^{-3}$)	0.512 and −0.866

[a] GooF $= \sqrt{\frac{\Sigma[w(F_o^2 - F_c^2)^2]}{(n-p)}}$ [b] $R_1 = \frac{\Sigma||F_o| - |F_c||}{\Sigma|F_o|}$; $wR_2 = \sqrt{\frac{\Sigma[w(F_o^2 - F_c^2)^2}{\Sigma[w(F_o^2)^2]}}$; $w = \frac{1}{\sigma^2(F_o^2) + (aP)^2 + bP}$; $P = \frac{2F_c^2 + \max(F_o^2, 0)}{3}$

Table 1.3: Crystallographic Data for ClBA·Et_2O

Identification code	P8_21123
Empirical formula, FW (g/mol)	$C_{18}H_{20}BClO$, 298.60
Color / Morphology	Colorless / Block
Crystal size (mm^3)	$0.200 \times 0.160 \times 0.140$
Temperature (K)	100(2)
Wavelength (Å)	0.71073
Crystal system, Space group	Orthorhombic, *Pbca*
Unit cell dimensions (Å, °)	$a = 14.4287(4)$, $\alpha = 90.000$
	$b = 14.0699(3)$, $\beta = 90.000$
	$c = 15.7970(4)$, $\gamma = 90.000$
Volume ($Å^3$)	3206.95(14)
Z	8
Density (calc., g/cm^3)	1.237
Absorption coefficient (mm^{-1})	0.234
$F(000)$	1264
Theta range for data collection (°)	2.398 to 34.970
Index ranges	$-22 \leq h \leq 23$, $-18 \leq k \leq 22$,
	$-25 \leq l \leq 24$
Reflections collected	73502
Independent reflections, R_{int}	6950, 0.0580
Completeness to $\theta_{\max}$ (%)	100.0
Absorption correction	Semi-empirical from equivalents
Refinement method	Full-matrix least-squares on F^2
Data / Restraints / Parameters	6950 / 0 / 192
Goodness-of-fit[a]	1.023
Final R indices[b] $[I > 2\sigma(I)]$	$R_1 = 0.0392$, $wR_2 = 0.0891$
R indices[b] (all data)	$R_1 = 0.0664$, $wR_2 = 0.1001$
Largest diff. peak and hole ($e \cdot Å^{-3}$)	0.414 and −0.318

[a] GooF $= \sqrt{\frac{\Sigma[w(F_o^2 - F_c^2)^2]}{(n-p)}}$ [b] $R_1 = \frac{\Sigma||F_o| - |F_c||}{\Sigma|F_o|}$; $wR_2 = \sqrt{\frac{\Sigma[w(F_o^2 - F_c^2)^2}{\Sigma[w(F_o^2)^2]}}$; $w = \frac{1}{\sigma^2(F_o^2) + (aP)^2 + bP}$; $P = \frac{2F_c^2 + \max(F_o^2, 0)}{3}$

1.5 Computational Details

1.5.1 Analysis of [MeBA][^{i}Pr$_2$AlMe$_2$] adduct

All calculations were performed using the ORCA 5.0.0 quantum chemistry package.[19] Geometry optimizations and frequency calculations were performed at the `B3LYP-D3/def2-TZVP` level of theory using keywords `B3LYP D3BJ def2-TZVP def2/J TightSCF RIJCOSX Opt NumFreq`. The optimized structure and tabulated bond lengths are displayed below.

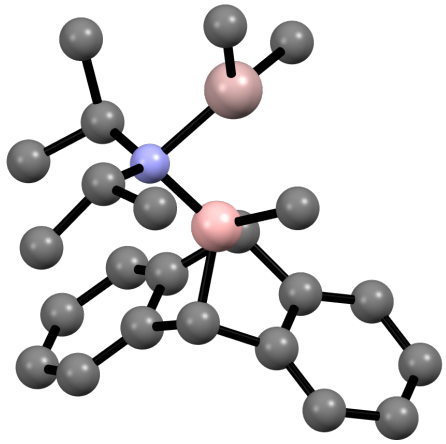

Figure 1-15: Calculated structure of the one-to-one complex of ^{i}Pr$_2$NBA and AlMe$_3$

Bond	Calculated Length (Å)	Σr_i^1 (Å)
B-N	1.635	1.56
Al-N	1.947	1.97
B-Me	1.707	1.60
Al-Me	2.312	2.01

Table 1.4: Relevant calculated bond lengths between boron, aluminum, nitrogen, and the bridging methyl carbon in the complex of ^{i}Pr$_2$NBA and AlMe$_3$. Respective sums of single bond covalent radii are given for comparison.[20]

Bibliography

[1] Wesley Transue, Liberation of low-coordinate phosphorus species from anthracene-based molecular precursors. Ph.D. thesis, Massachusetts Institute of Technology, 2018.

[2] Fagan, P. J.; Burns, E. G.; Calabrese, J. C. Synthesis of boroles and their use in low-temperature Diels-Alder reactions with unactivated alkenes. *Journal of the American Chemical Society* **1988**, *110*, 2979–2981.

[3] Braunschweig, H.; Maier, J.; Radacki, K.; Wahler, J. Ring Expansion of 7-Boranorbornadienes by Coordination with an N-Heterocyclic Carbene. *Organometallics* **2013**, *32*, 6353–6359.

[4] Fan, C.; Piers, W. E.; Parvez, M.; McDonald, R. Divergent Reactivity of Perfluoropentaphenylborole with Alkynes. *Organometallics* **2010**, *29*, 5132–5139.

[5] Lindl, F.; Guo, X.; Krummenacher, I.; Rauch, F.; Rempel, A.; Paprocki, V.; Dellermann, T.; Stennett, T. E.; Lamprecht, A.; Brückner, T.; Radacki, K.; Bélanger-Chabot, G.; Marder, T. B.; Lin, Z.; Braunschweig, H. Rethinking Borole Cycloaddition Reactivity. *Chemistry – A European Journal* **2021**, *27*, 11226–11233.

[6] Ge, F.; Kehr, G.; Daniliuc, C. G.; Erker, G. Borole Formation by 1,1-Carboboration. *Journal of the American Chemical Society* **2014**, *136*, 68–71.

[7] Velian, A.; Cummins, C. C. Facile Synthesis of Dibenzo-7 ^{3} -phosphanorbornadiene Derivatives Using Magnesium Anthracene. *Journal of the American Chemical Society* **2012**, *134*, 13978–13981.

[8] Transue, W. J.; Velian, A.; Nava, M.; García-Iriepa, C.; Temprado, M.; Cummins, C. C. Mechanism and Scope of Phosphinidene Transfer from Dibenzo-7-phosphanorbornadiene Compounds. *Journal of the American Chemical Society* **2017**, *139*, 10822–10831.

[9] Keisel, K.; Noth, H.; Polborn, K. CCDC 168347: Experimental Crystal Structure Determination. 2001.

[10] Höbel, U.; Nöth, H.; Prigge, H. Beiträge zur Chemie des Bors, 165. Diisopropyl- und Di- *tert* -butylboran-Derivate. *Chemische Berichte* **1986**, *119*, 325–337.

[11] Pangborn, A. B.; Giardello, M. A.; Grubbs, R. H.; Rosen, R. K.; Timmers, F. J. Safe and Convenient Procedure for Solvent Purification. *Organometallics* **1996**, *15*, 1518–1520.

[12] Williams, D. B. G.; Lawton, M. Drying of Organic Solvents: Quantitative Evaluation of the Efficiency of Several Desiccants. *The Journal of Organic Chemistry* **2010**, *75*, 8351–8354.

[13] Ordyszewska, A.; Szynkiewicz, N.; Perzanowski, E.; Chojnacki, J.; Wiśniewska, A.; Grubba, R. Structural and spectroscopic analysis of a new family of monomeric diphosphinoboranes. *Dalton Transactions* **2019**, *48*, 12482–12495.

[14] Armarego, W. L. F.; Chai, C. L. L. *Purification of laboratory chemicals*, 6th ed.; Elsevier/BH: Oxford, 2009; OCLC: 424595775.

[15] Fulmer, G. R.; Miller, A. J. M.; Sherden, N. H.; Gottlieb, H. E.; Nudelman, A.; Stoltz, B. M.; Bercaw, J. E.; Goldberg, K. I. NMR Chemical Shifts of Trace Impurities: Common Laboratory Solvents, Organics, and Gases in Deuterated Solvents Relevant to the Organometallic Chemist. *Organometallics* **2010**, *29*, 2176–2179.

[16] Sheldrick, G. M. SHELXT – Integrated space-group and crystal-structure determination. *Acta Crystallographica Section A Foundations and Advances* **2015**, *71*, 3–8.

[17] Müller, P.; Herbst-Irmer, R.; Spek, A. L.; Schneider, T. R.; Sawaya, M. R. *Crystal Structure Refinement*; Oxford University Press, 2006.

[18] Müller, P. Practical suggestions for better crystal structures. *Crystallography Reviews* **2009**, *15*, 57–83.

[19] Neese, F. Software update: The ORCA program system—Version 5.0. *WIREs Computational Molecular Science* **2022**, *12*.

[20] Pyykkö, P. Additive Covalent Radii for Single-, Double-, and Triple-Bonded Molecules and Tetrahedrally Bonded Crystals: A Summary. *The Journal of Physical Chemistry A* **2015**, *119*, 2326–2337.

Chapter 2

Molecular Precursors for the Generation of Free Monomeric Oxoboranes

2.1 Introduction

Oxoboranes (R-B=O) are a class of low-coordinate reactive intermediates that have attracted significant research interest in the last several decades due to their novel reactivity, involvement in chemical processes such as the carbonylation of boranes to form ketones[1,2] and the recently reported phospha-bora-Wittig reaction,[3] and poorly studied electronic structure. Although a wide variety of oxoboranes have been generated and characterized in the gas phase or matrix isolation,[4–17] generation methods such as high temperature ($>$ 500 °C), plasma discharge, and laser ablation are unselective, poorly scalable, and synthetically unuseful. The first method for the generation of a free monomeric oxoborane in solution came from a 1985 study by Bernd Pachaly and Robert West, who demonstrated the synthesis of a 1,3-dioxa-2,4-diboretane, formally an oxoborane dimer, and its photolysis for the transient generation of the monomer.[18] A decade later, Okazaki and coworkers introduced the first solution-state thermal method via a 1,3,2,4-dithiastannaboretane that underwent

thermolysis to form a transient thioxoborane (R-B=S).[19] Treatment of the stannacycle with dimethyl sulfoxide led to the generation of the oxoborane analog,[20] and the same framework was further adapted for the generation of a free selenoxoborane (R-B=Se).[21] However, both of these approaches are dependent on the use of highly sterically encumbering R-groups, namely supermesityl (2,4,6-tri-*tert*-butylphenyl) and Tbt (2,4,6-tris(bis(trimethylsiyl)methyl)phenyl), limiting the versatility and tunability of the generated species and their synthetic applications. Moreover, the use of toxic organotin reagents is not preferred in modern chemical synthesis.

Nonetheless, little progress in the area of generating and studying free fragments has been over the last two decades; others have instead turned towards investigating the chemistry of isolable Lewis acid and/or base-stabilized oxoboranes, the first of which was reported in 2005 by Cowley and coworkers.[22] Since then, numerous neutral, anionic, and cationic complexes containing a B=E (E = O, S, Se, Te) multiple bond supported by a variety of ligands have been reported,[23–35] with an especially notable example being the recently introduced bidentate amido imidazoline-2-imine ligand (AmIm) which was found to be capable of stabilizing B=E double bonds with all four chalcogens in neutral complexes without the need for a Lewis acid.[36] Lastly, there has been substantial interest in studying the properties of exotic ligands isoelectronic with carbon monoxide, such as BO^-. To date, only one such metal boronyl complex has been reported and was prepared by Braunschweig and coworkers via oxidative addition of $Me_3SiOBBr_2$ to bulky and Lewis basic $(Cy_3P)_2Pt(0)$ and subsequent Me_3SiBr elimination.[37] Thus, although the topic of ligand-stabilized boron-chalcogen multiply bonded systems has been quite well studied and discussed overall, the chemistry of free monomeric oxoborane derivatives remains largely unexplored.

2.2 Mono-oxidation of Dibenzo-7-boranorbornadienes

We envisioned that oxidation of the RBA molecules described in the previous chapter would offer a platform for the cleaner and more versatile generation of free oxoboranes in solution under relatively mild conditions. Upon examination of the literature, it

was found that the mono-oxidation of bicyclic boranes using trimethylamine N-oxide is an established and well-studied procedure developed by Soderquist and Najafi.[38] This method is particularly convenenient for our goal given its selectivity for ring B-C bond oxidation: in the case of B-alkyl-9-borabicyclo[3.3.1]nonane, the 9-oxa-10-borabicyclo[3.3.2]decane is formed exclusively due to the preference for the amine to leave anti-periplanar to the migrating B-C bond.[38]

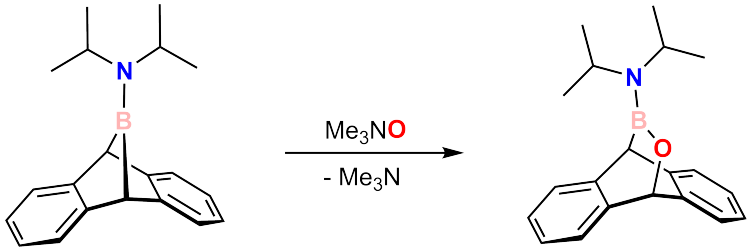

Figure 2-1: Synthesis of $^{i}Pr_2$NBOA via oxidation of $^{i}Pr_2$NBA with an amine oxide.

Treatment of $^{i}Pr_2$NBA with Me_3NO in tetrahydrofuran solution did indeed proceed well to form the anthracene-based [2.2.2] bicyclic borinate ester $^{i}Pr_2$NBOA in good yields, typically in the range of 70 to 80%. The structure was confirmed by its ^{11}B NMR resonance, shifted approximately 10 ppm upfield from $^{i}Pr_2$NBA to δ 30.8 ppm, and the presence of two distinct bridgehead proton signals in the ^{1}H spectrum, in addition to an x-ray diffraction experiment using single crystals grown from diethyl ether solution (Fig. 2-2).

We immediately turned towards investigating the thermal stability of this compound in solution and observed the slow formation of trimeric $(^{i}Pr_2NBO)_3$ via ^{11}B NMR upon heating to 80 °C in benzene solution. Periodic measurements on this sample over the course of five days confirmed that this reaction proceeds according to first-order kinetics, indicative of a unimolecular rate-determining step (Section 2.3.3). To the best of our knowledge, this entails the first method for the on-demand unimolecular generation of a free oxoborane monomer under typical laboratory conditions.

Separately, we carried out quantum chemical calculations for further insight into the mechanism of thermal fragmentation. Geometry optimizations and frequencies of

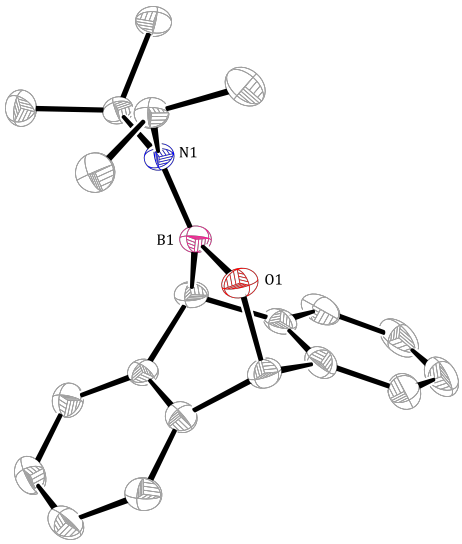

Figure 2-2: Molecular structure $^{i}Pr_2NBOA$, shown with ellipsoids at the 50% probability level and hydrogen atoms omitted for clarity. Selected interatomic distances (Å): B1-O1 1.405(3), N1-B1 1.395(3), B1-C1 1.611(3), O1-C8 1.464(2).

relevant species were calculated by DFT (B3LYP-D3BJ/def2-TZVP level of theory) and single point energies for all structures were calculated using the domain-based local pair natural orbital coupled-cluster method with singles, doubles, and perturbative triples excitation (DLPNO-CCSD(T)) using TightPNO settings and the cc-pVTZ basis set. The results indicated that the reaction occurs via concerted elimination of $^{i}Pr_2NBO$ and anthracene, with further details available in Section 2.5.1.

Interested to test the ability of $^{i}Pr_2NBOA$ to act as an oxoborane transfer reagent for use in synthesis, we conducted reactions in the presence of chemical traps (summarized in Fig. 2-3). Thermolysis in the presence of mesitonitrile N-oxide or ethyl vinyl ketone led to formation of the corresponding [3+2] cycloadducts. Moreover, it was noted that $^{i}Pr_2NBOA$ was prone to decomposition upon exposure to light during storage in the glovebox, so photochemical fragmentation was carried out in the presence of pinacolone and found to form the [2+2] cycloadduct.

Unfortunately, however, the transfer of $^{i}Pr_2NBO$ has thus far been entirely limited to substrates that lead to B-O bond formation, such as those listed above, and it is believed that this is a very strong thermodynamic driving force. No new reactivity was observed upon thermolysis at 80 to 100 °C in the presence of the azophosphine

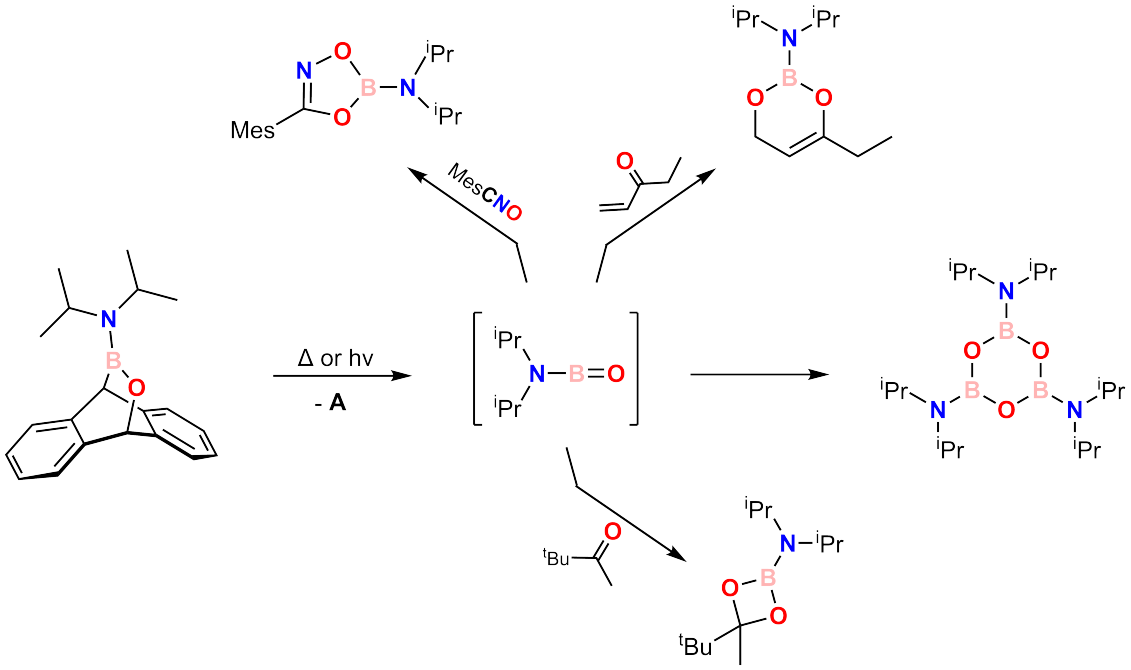

Figure 2-3: Summary of the behavior of $^{i}Pr_2NBOA$ upon thermolysis or photolysis and accessible oxoborane cycloaddition chemistry.

$TolNNPPh_2$[39] or in neat 2,3-dimethyl-1,3-butadiene or 1,3-cyclohexadiene, for instance. Even in the case of B-O bond-forming substrates, $(^{i}Pr_2NBO)_3$ formation competes heavily with the cycloaddition reaction and is formed in significant quantities unless a large stoichiometric excess of the trap is used.

It is hypothesized that the lower than expected reactivity of $^{i}Pr_2NBO$ is explained in large part due to the strongly electron-donating amino substituent on boron – it may be noted that $^{i}Pr_2NBOA$ displays a B-N bond length of 1.395 Å, compared to 1.375 in $^{i}Pr_2NBA$, and thus barely longer than the sum of double bond covalent radii.[40] In contrast to previous computational studies indicating the presence of a boron-oxygen triple bond in free H_2NBO,[41] linear $^{i}Pr_2NBO$ seems to be better described as having boron-nitrogen and boron-oxygen double bonds which, although still unstable, is far less reactive than anticipated. Consistent with this description, $^{i}Pr_2NBO$ was not found to react readily with dicobalt octacarbonyl, where it was initially thought that a triply bonded BO π-system could bind to the cobalt centers as alkynes are well known to do.[42] Naturally, we next wondered if the oxoborane could

bind in an η^2 fashion to a metal center and treated $^{i}Pr_2NBOA$ with $(Ph_3P)_2Pt(C_2H_4)$ at 100 °C in toluene solution. Although no new ^{11}B NMR signals other than boroxine could be identified, heating for 24 hours led to the release of free ethylene into solution and formation of a bright red species that is only moderately soluble in toluene but soluble in dichloromethane. The full identity of this material remains unknown, as single crystals of suitable quality for x-ray diffraction experiments could not yet be grown, however the presence of triphenylphosphine and platinum was confirmed by mass spectrometry. Lastly, we attempted to treat $^{i}Pr_2NBOA$ with the nucleophilic metal complex $K[CpFe(CO)_2]$, or FpK, but no reactivity was observed, again highlighting the relatively high degree of stability offered to the fragment by the amino substituent. It is expected that the synthesis of other RBOA containing other weaker- or non-electron-donating substituents on boron will unlock a greater range of novel reactivity, pending further progress on the synthesis of RBA molecules described in Chapter One.

Given the promising reactivity of $^{i}Pr_2NBO$ towards oxygen-containing substrates, we were interested to investigate how it would interact with carbon dioxide. Initially hoping to form a covalent boron carbonate, which to the best of our knowledge has never been reported, we carried out the photolysis of $^{i}Pr_2NBOA$ in toluene solution at 254 nm under an atmosphere of CO_2. Interestingly, only the presence of boroxine could be noted by NMR, however a significant amount of precipitate had formed over the course of the reaction. Although easily isolated, the analysis of this new material has been made difficult by its apparent insolubility in most organic solvents. Samples were prepared in acetonitrile and dimethyl sulfoxide. Although no signal was observed in MeCN, there was indeed a boron-containing species present that was slightly soluble in DMSO; this observation confirmed that there was a new species in addition to boroxine. Nonetheless, the infrared spectrum of the isolated material notably lacked a carbonyl stretching frequency. Based on this and the propensity of oxoboranes for reacting with B-O bond-forming substrates in solution, it was hypothesized that the targeted boron carbonate may form transiently before addition of a second equivalent of $^{i}Pr_2NBO$, yielding a diboron orthocarbonate (Fig. 2-4).

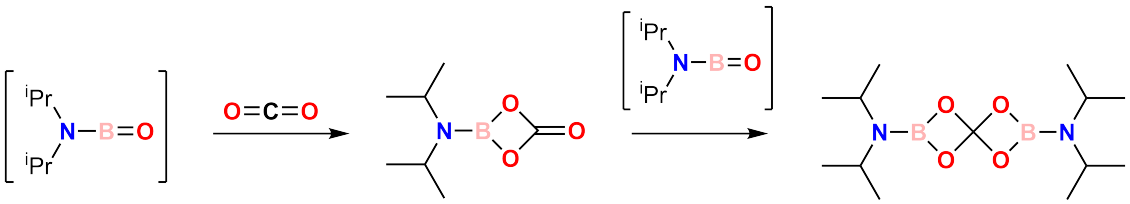

Figure 2-4: Current hypothesis for the reactivity of $^{i}Pr_2NBO$ towards CO_2.

Upon survey of the literature, we found that very similar reactivity of an unstable silanone has been previously reported (Fig. 2-5).[43]

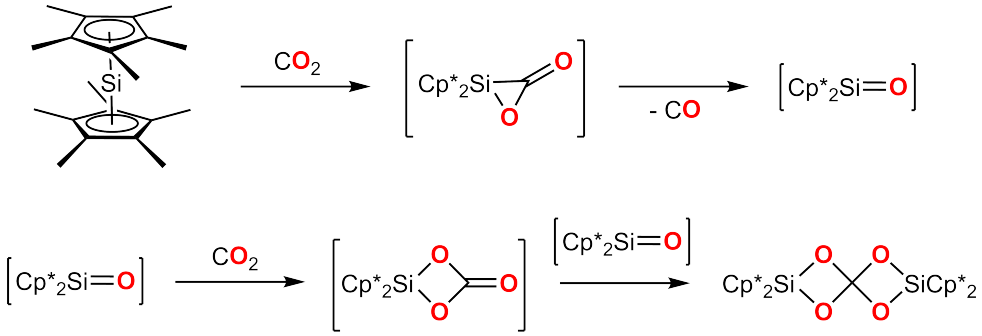

Figure 2-5: Summary of previous literature discussing reactivity of a transient silanone exhibiting reactivity analagous to that proposed to occur between $^{i}Pr_2NBO$ and CO_2.[43]

In an effort to better support our above hypothesis, the solid material was treated with D_2O. It was expected that the boron ester bonds would be easily hydrolyzed to potentially form highly unstable orthocarbonic acid, $(HO)_4C$, which would instantaneously convert to carbon dioxide and water (Fig. 2-6).

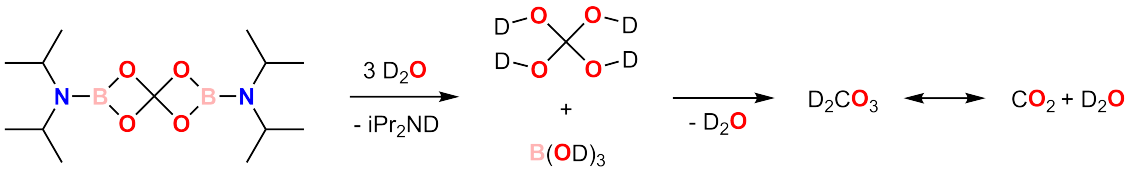

Figure 2-6: Proposed method for indirect analysis of the insoluble material, putatively assigned to be the boron orthocarbonate $(^{i}Pr_2NBO)_2(CO_2)$.

Indeed $B(OD)_3$ and free $^{i}Pr_2ND$ could be identified by ^{11}B and ^{1}H NMR spectroscopy (see Section 2.3.6). Although this particular result is consistent with the proposed structure, it is not direct confirmation and further experiments involving

^{13}C labeling are planned. Based on the outcome of these studies, this branch of oxoborane reactivity may allow for indirect access to an interesting area of exotic carbonate chemistry.

2.2.1 Attempts to access electrophilic oxoboranes

In an effort to pursue the chemistry of entirely unstabilized oxoboranes that might display particularly interesting reactivity using the RBA precursors that have been successfully isolated up to this point, we wondered if mono-oxidation of ClBA·Et_2O could be achieved. The target species, ClBO, has been studied in the gas phase,[17] however it is known to be extremely unstable; even the trimer, trichloroboroxine or $(ClBO)_3$, is known to be unisolable as a solid and has been described to decompose rapidly upon condensation from the gas phase.[44] In 2017, Rivard and coworkers isolated the first stable push-pull complexes of ClBO and HOBO between an N-heterocyclic carbene and $B(C_6F_5)_3$ and demonstrated its ability to controllably activate C-F and Si-O bonds. However, other than this single study, little progress has been made in the area of electrophilic oxoboranes.

Unfortunately, a method for the isolation of ClBOA or one of its adducts has not yet been found, however interesting reactivity has been observed. As to avoid the presence of free Lewis basic NMe_3 in solution, we turned towards iodosylbenzene (PhIO) as an alternative O-transfer reagent. Addition of PhIO to a dichloromethane solution of ClBA·Et_2O gave a heterogenous yellow solution. An NMR analysis showed loss of boron signal and free anthracene. This experiment was repeated at -35 °C in the glovebox freezer: Interestingly, after filtration of the cold crude mixture into an NMR tube, a precipitate consisting primarily of anthracene formed in the tube within minutes. ^{11}B NMR revealed the presence of a broad resonance at δ 37.2 ppm, potentially corresponding to ClBOA (^{11}B NMR calcd. δ 43.6 ppm, though it is also feasible for the observed species to be a diethyl ether adduct) or $(ClBO)_3$, however the latter compound is not expected to be stable or soluble enough for observation. ^{1}H NMR indicated the presence of a singlet at δ 6.21 ppm that could correspond to the oxygen-adjacent bridgehead proton, but further study of this species has been

hindered by its rapid decomposition under normal conditions. Thus, although the thermal barrier to unimolecular anthracene elimination is sufficiently high (calcd. 29.3 kcal/mol) for isolation, it is currently hypothesized that ClBOA forms at low temperature before decomposing according to an unknown reaction pathway: it may be very light sensitive and/or lose anthracene via an intermolecular reaction due to the lack of steric protection. Other synthetic routes towards similar electrophilic oxoborane precursors are currently being explored.

2.3 Experimental Details

2.3.1 General Information

Except as otherwise noted, all manipulations were performed in a Vacuum Atmospheres model MO-40M glovebox under an inert atmosphere of purified N_2. All solvents were obtained anhydrous and oxygen-free by bubble degassing (Ar), passage through columns of alumina using a solvent purification system (Pure Process Technology, Nashua, NH),[45] and storage over 4.0 Å molecular sieves.[46] Deuterated solvents were purchased from Cambridge Isotope Labs and degassed by three freeze-pump-thaw cycles and stored over 4 Å molecular sieves for at least 48 h prior to use. Diatomaceous earth (EM Science) and 4 Å molecular sieves were dried by heating above 200 °C under dynamic vacuum for at least 48 h prior to use. All glassware was dried in an oven for at least two hours at temperatures greater than 150 °C.

Mesitonitrile N-oxide (MesCNO)[47] and [(η^5-C_5H_5)Fe$(CO)_2$]K (FpK)[48] were prepared according to literature procedures. Pinacolone (Sigma-Aldrich) and 1-penten-3-one (Sigma-Aldrich) were degassed by three freeze-pump-thaw cycles and stored over 4 Å molecular sieves prior to use. Trimethylamine N-oxide (Sigma-Aldrich) was made anhydrous by heating at 105 °C under dynamic vacuum for 24 hrs prior to storage in the glovebox. Acenapthene (Sigma-Aldrich), $(Ph_3P)_2Pt(C_2H_4)$ (Sigma-Aldrich), octacarbonyldicobalt (Alfa-Aesar), Kryptofix 222 (Sigma-Aldrich), iodosobenzene (TCI Chemicals), and carbon dioxide (Airgas) were used as received.

NMR spectra were obtained on a Bruker Avance 400 instrument equipped with a Magnex Scientific or with a SpectroSpin superconducting magnet or on a Bruker Avance 500 instrument equipped with a Magnex Scientific or with a SpectroSpin superconducting magnet. ^{1}H and ^{13}C NMR spectra were referenced internally to residual solvent signals.[49] ^{11}B and ^{31}P NMR spectra were externally referenced to 15% $BF_3{\cdot}Et_2O$ in $CDCl_3$ (0 ppm) and 85% H_3PO_4 (0 ppm), respectively.

High resolution mass spectral (HRMS) data were collected using a Jeol AccuTOF 4G LC-Plus mass spectrometer equipped with an Ion-Sense DART source. Data were calibrated to a sample of PEG-600 and were collected in positive-ion mode. Samples were prepared in pentane or dichloromethane (ca. 10 μM concentration) and were briefly exposed to air before being placed in front of the DART source.

Photochemical reactions were performed using a Rayonet photochemical reactor RPR-200 (Southern New England Ultra Violet Company) loaded with 16 RPR-2537A lamps, each emitting ca. 35 W at 253.7 nm.

2.3.2 Synthesis of $^{i}Pr_2NBOA$

A 250 mL flask was loaded with ^{i}Pr2NBA (1.5 g, 5.19 mmol, 1 equiv) and THF (100 mL). With vigorous stirring, solid Me_3NO (393 mg, 5.24 mmol, 1.01 equiv) was added in a single portion. The vessel was placed under 1 atm of nitrogen on the Schlenk line and the heterogeneous mixture was stirred for 16 hours. Volatiles were removed under reduced pressure and the flask returned to the glovebox. The crude material was resuspended in Et_2O (50 mL) and filtered through a medium sintered frit with a one inch plug of celite and activated charcoal. The filtrate was concentrated and the solids obtained recrystallized from a minimal amount of ether at -35 ℃ to afford ^{i}Pr2NB(OA as a colorless solid (1.2 g, 3.93 mmol, 76%). ^{1}H NMR (400 MHz, Benzene-d_6, 25 °C) δ 7.31 - 7.21 (m, 2H), 7.18 - 7.15 (m, 2H), 7.01 - 6.91 (m, 4H), 6.07 (s, 1H), 4.34 (s, 1H), 3.65 (hept, J = 6.8 Hz, 1H), 3.37 (hept, J = 7.0 Hz, 1H), 1.16 (d, J = 6.9 Hz, 6H), 0.88 (d, J = 6.8 Hz, 6H) ppm. ^{11}B NMR (128 MHz, Benzene-d_6, 25 °C) δ 30.8 ppm.

2.3.3 Kinetics of $^{i}Pr_2NBO$ Release

Solid $^{i}Pr_2NBOA$ (20 mg, 0.066 mmol, 1.0 equiv) was weighed out in a small vial and dissolved in deuterated benzene (0.7 mL). Acenaphthene (5.1 mg, 0.033 mmol, 0.50 equiv) was added as an internal standard, and the homogeneous solution was transferred to a J Young tube. The sample was heated in an 80 °C oil bath and the progress of the reaction was monitored periodically over five days by quantitative ^{1}H NMR spectroscopy (Fig. 2-7). Spin-lattice decay constants (T_1) were measured using an inversion-recovery pulse sequence and T_1 times of 3 s, 5 s, and 2 s were found for the ethylene proton resonance of acenapthene (2.98 ppm in benzene-d_6) and the bridgehead proton resonance on the oxygen side (6.07 ppm in benzene-d_6) and boron side (4.34 ppm in benzene-d_6) of $^{i}Pr_2NBOA$, respectively. The relaxation delay was set to 30 s to obtain a quantitative ^{1}H NMR spectrum.

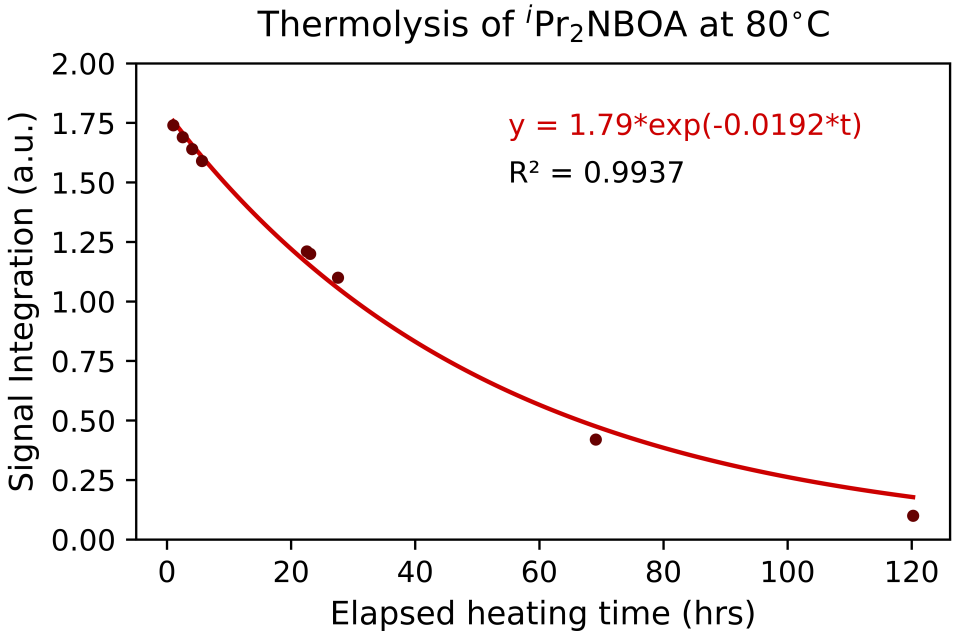

Figure 2-7: Kinetics of $^{i}Pr_2NBOA$ thermolysis at 80 °C. The plot of concentration fits well to exponential decay ($R^2 = 0.9937$), consistent with a first-order rate law.

2.3.4 Chemical trapping of $^{i}Pr_2NBO$

The following general procedure was followed: Solid $^{i}Pr_2NBOA$ was weighed out in a small vial and dissolved in benzene or toluene (concentrations of 10-20 mg/mL). The chemical trap (1 to 10 equiv) was separately weighed out and added to the solution with stirring. The reaction mixture was transferred to either a J Young tube or Schlenk tube, then the vessel sealed and removed from the glovebox. [3+2] cycloadditions with MesCNO and ethyl vinyl ketone were carried out via heating in an 80 to 100 °C oil bath. The [2+2] cycloaddition with pinacolone was carried out in a Rayonet photoreactor equipped with 254 nm UV bulbs. The progress of all reactions were monitored via heteronuclear NMR. These cycloadducts have not yet been isolated in their pure forms primarily due to the challenge posed by separation from the significant quantities of $(^{i}Pr_2NBO)_3$ formed, given its good solubility in organic solvents. Nonetheless, related oxoborane cycloadditions have been previously reported.[18,20]

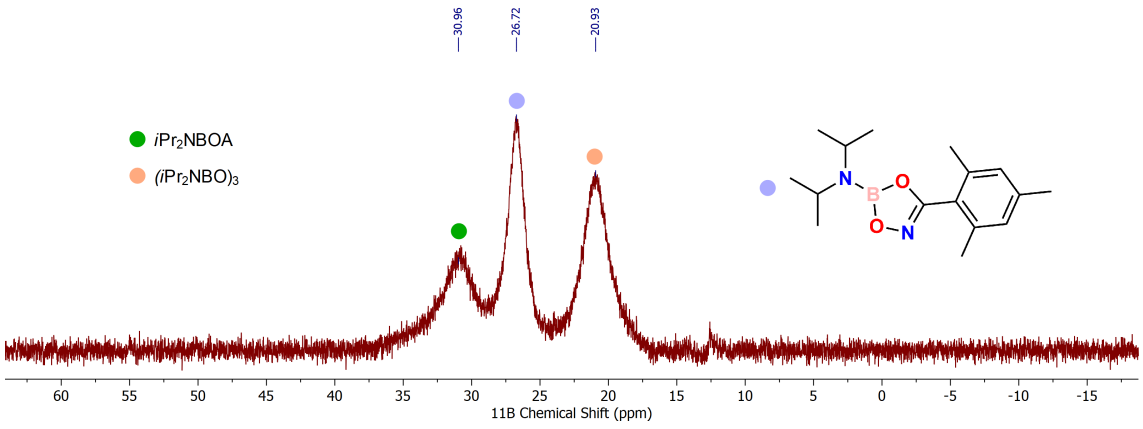

Figure 2-8: ^{11}B NMR (128 MHz, Benzene-d_6, 25 °C) of a solution of stoichiometric $^{i}Pr_2NBOA$ and MesCNO after heating at 80 °C for two days.

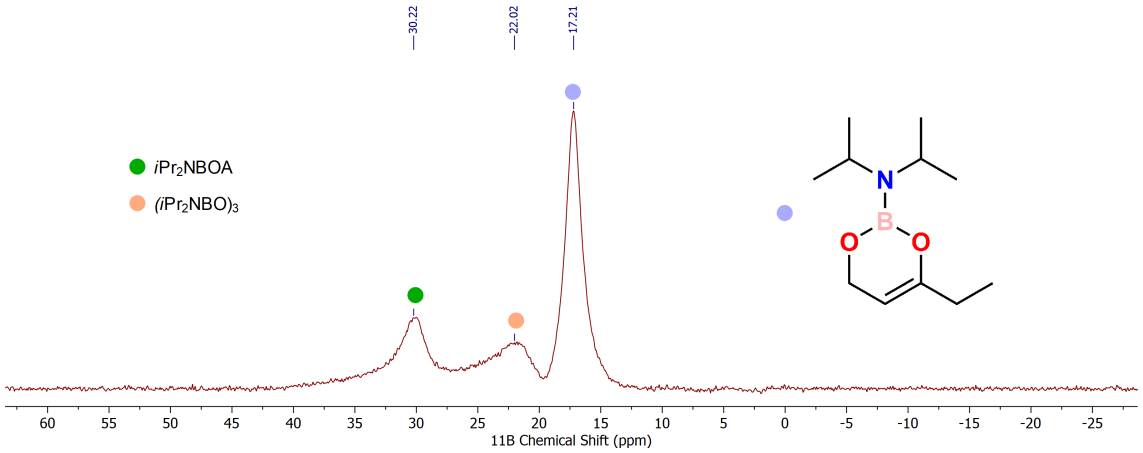

Figure 2-9: ^{11}B NMR (128 MHz, Toluene-H, 25 °C) of a solution of ^{i}Pr$_2$NBOA and 10 equivalents of ethyl vinyl ketone after heating at 100 °C 16 hours.

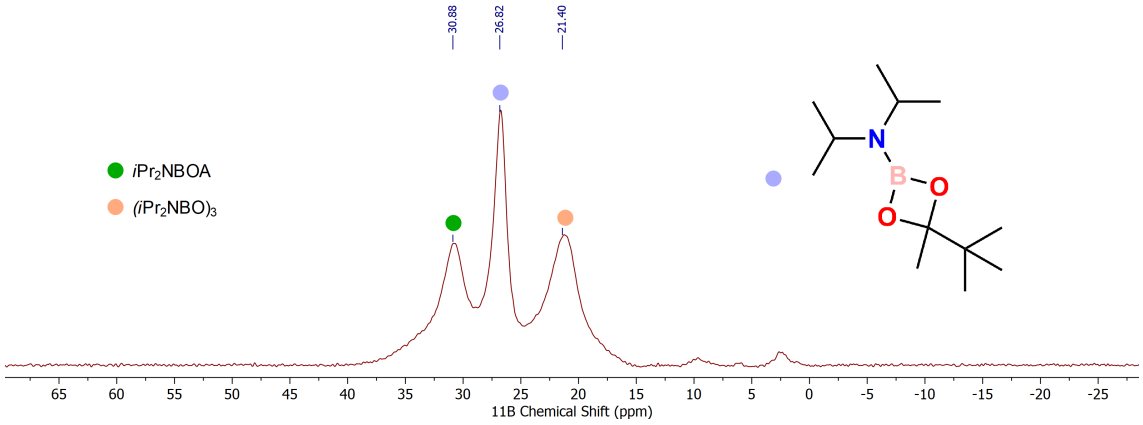

Figure 2-10: ^{11}B NMR (128 MHz, Toluene-H, 25 °C) of a solution of stoichiometric ^{i}Pr$_2$NBOA and pinacolone after photolysis with 254 nm light for 30 minutes.

2.3.5 Treatment of ^{i}Pr$_2$NBOA with Transition Metal Complexes

With $(Ph_3P)_2Pt(C_2H_4)$

^{i}Pr$_2$NBOA (10 mg, 0.033 mmol, 1.0 equiv) was dissolved in toluene (0.7 mL) in a small vial. Solid $(Ph_3P)_2Pt(C_2H_4)$ (25 mg, 0.033 mmol, 1.0 equiv) was added and the mixture agitated to dissolve. The homogeneous light yellow solution was transferred to a J Young tube and placed in a 100 °C oil bath in the fumehood, quickly turning it deep red in color. The tube was heated for 16 hours then allowed to cool, after

which point a significant quantity of bright red precipitate had settled at the bottom. The sample was returned to the glovebox and the solids collected on glass microfiber filter paper, then washed with a small amount of pentane (1 mL) before transferring to a vial for storage and further analysis. Very little information could be obtained by NMR, as the only major ^{11}B signal matched that of (^{i}Pr$_2$NBO)$_3$ and the ^{31}P NMR spectrum had a very poor signal to noise ratio. Mass spectrometry confirmed the presence of triphenylphosphine and boroxine. A black residue remained on the capillary after the experiment, which was presumed to be metallic platinum. Single crystals of suitable quality for structure determination could not be grown under crystallization conditions that have been attempted thus far.

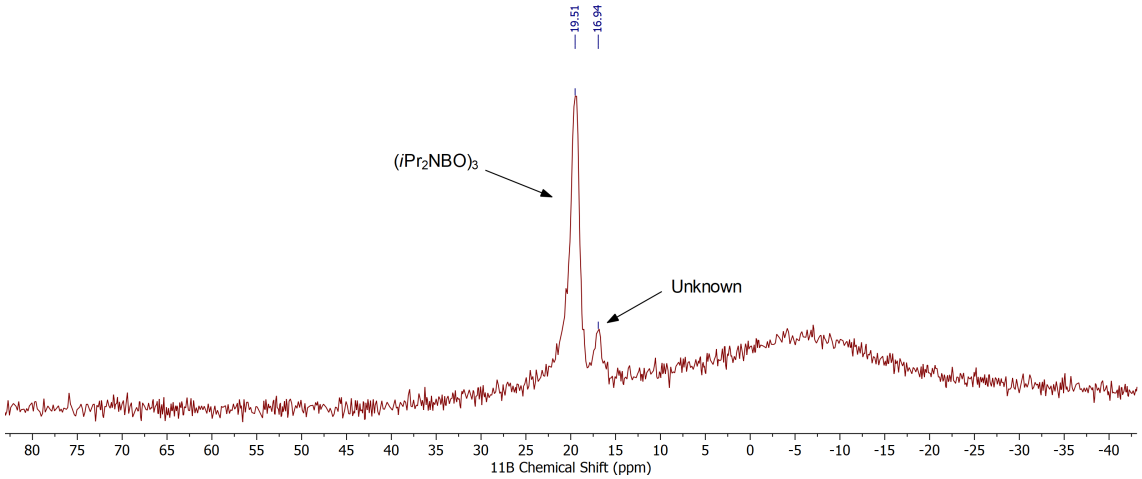

Figure 2-11: ^{11}B NMR (160 MHz, Toluene-H, 85 °C) spectrum of the red solids isolated after thermolysis of ^{i}Pr$_2$NBOA in the presence of (Ph$_3$P)$_2$Pt(C$_2$H$_4$).

With FpK

^{i}Pr$_2$NBOA (10 mg, 0.0328 mmol, 1.0 equiv) was dissolved in benzene (0.7 mL) in a small vial and solid FpK (7 mg, 0.0324 mmol, 1.0 equiv) was added. To the stirring solution was added Kryptofix 222 (12.3 mg, 0.327 mmol, 1.0 equiv), turning the solution orange as the FpK was solvated. An initial ^{11}B NMR experiment confirmed that no reaction had occured at room temperature, so the sample was transferred to a J Young tube, removed from the glovebox, and heated in an 80 °C oil bath overnight.

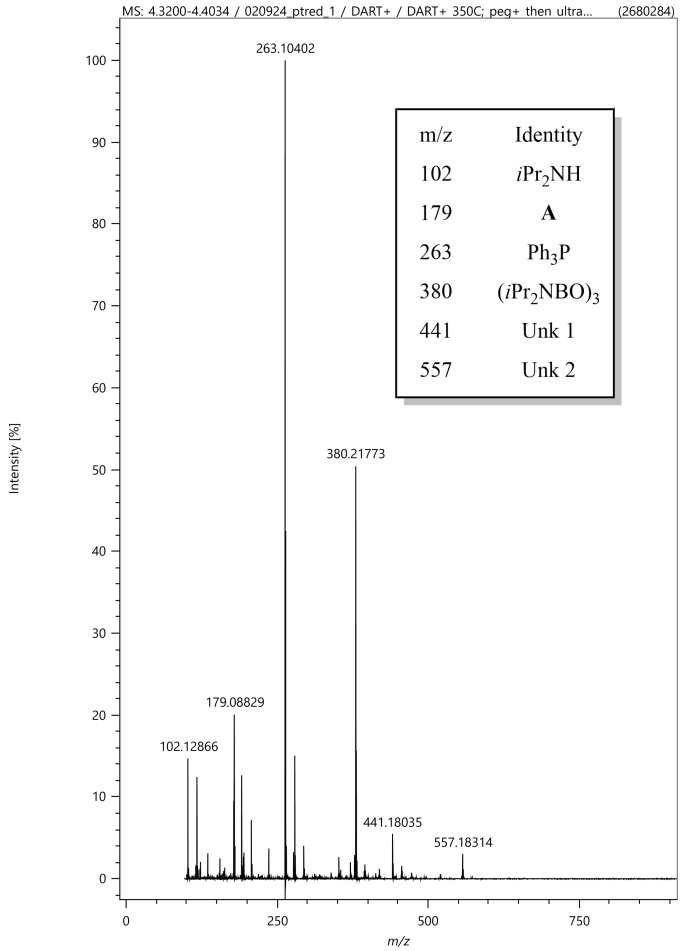

Figure 2-12: DART-HRMS analysis of the red solids isolated after thermolysis of $^{i}Pr_2NBOA$ in the presence of $(Ph_3P)_2Pt(C_2H_4)$.

^{11}B NMR indicated that there was a very small new resonance at δ 1.7 ppm, however $(^{i}Pr_2NBO)_3$ was evidently preferentially formed over binding to iron.

With $Co_2(CO)_8$

To a solution of $^{i}Pr_2NBOA$ (16 mg, 0.0525 mmol, 1.0 equiv) in benzene (0.7 mL) was added $Co_2(CO)_8$ (18 mg, 0.0526 mmol, 1.0 equiv). The dark solution was transferred to a J Young tube, and an initial NMR analysis confirmed that no reaction had occurred. Given the thermal instability of dicobalt octacarbonyl,[50] the sample was exposed to 254 nm UV light in a Rayonet photoreactor with a cooling fan for the generation of free oxoborane, rather than heating. After two hours, a new small

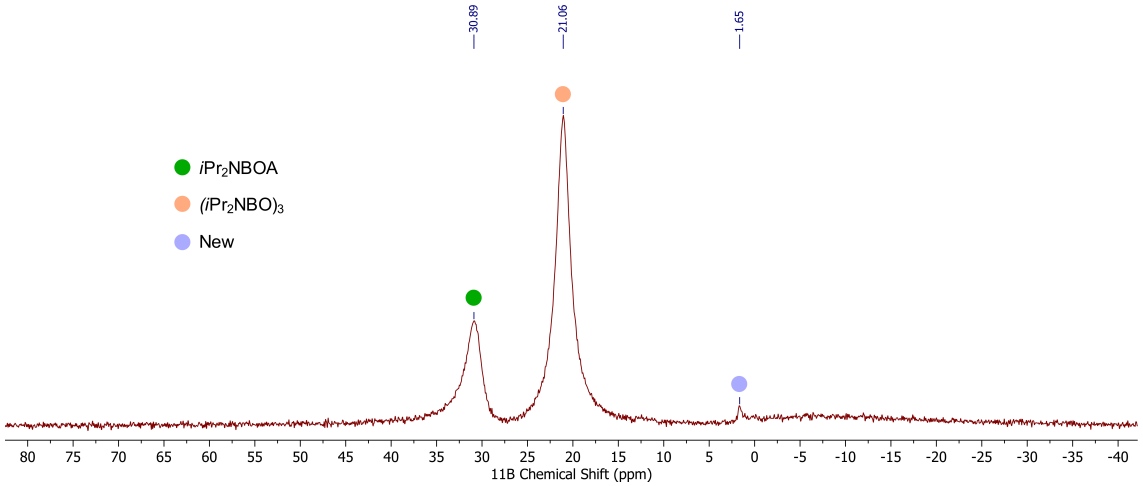

Figure 2-13: ^{11}B NMR (160 MHz, Benzene-d_6, 25 °C) spectrum of the reaction mixture after thermolysis of ^{i}Pr$_2$NBOA in the presence of Fp[K(2.2.2)crypt].

^{11}B resonances could be observed at δ 26.8 ppm, however the boroxine formed preferentially and was observed as the major product; the new signal did not continue to grow upon further photolysis. The ^{1}H NMR spectrum was severely broadened.

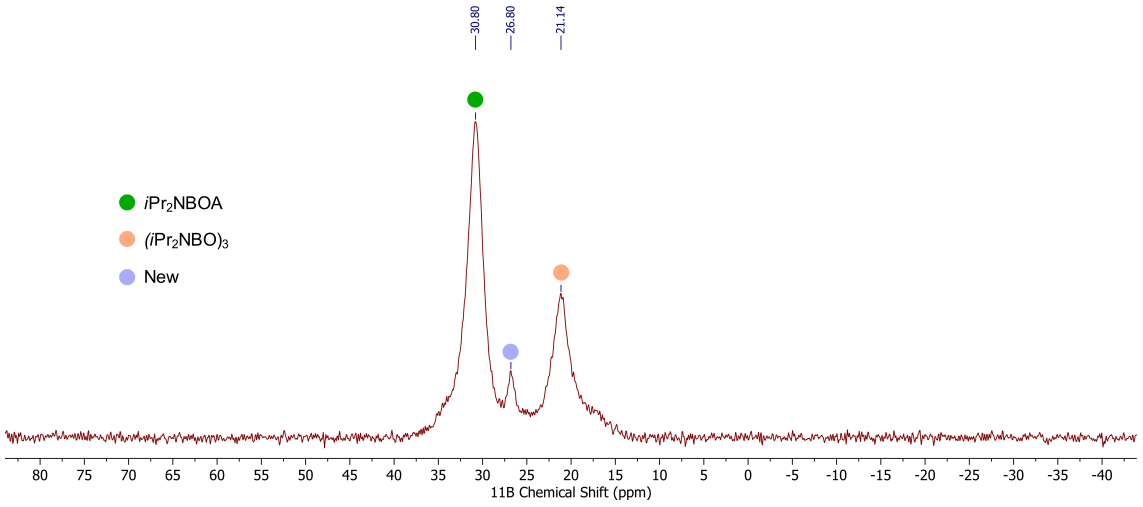

Figure 2-14: ^{11}B NMR (160 MHz, Benzene-d_6, 25 °C) spectrum of the reaction mixture after photolysis of ^{i}Pr$_2$NBOA in the presence of $Co_2(CO)_8$.

2.3.6 Photolysis of $^{i}Pr_2NBOA$ in the presence of CO_2

A J Young tube was charged with $^{i}Pr_2NBOA$ (40 mg, 0.13 mmol) and toluene (1 mL). The tube was capped, removed from the glovebox, and subject to five freeze-pump-thaw cycles on the Schlenk line in order to degas the solution. The tube was backfilled with CO_2 gas, then the cap tightened, before placing it in a Rayonet photoreactor and exposing to 254 nm UV light for six hours. The vessel was briefly sonicated to knock the precipitate formed off of the inner wall, then returned to the glovebox where the precipitate was collected on glass filter paper in a pipette filter. The solids were washed thoroughly with pentane (5 mL) and DCM (3 mL), then transferred to a small vial and allowed to dry by evaporation of the solvent. After this process, 14.3 mg of the colorless insoluble product was obtained.

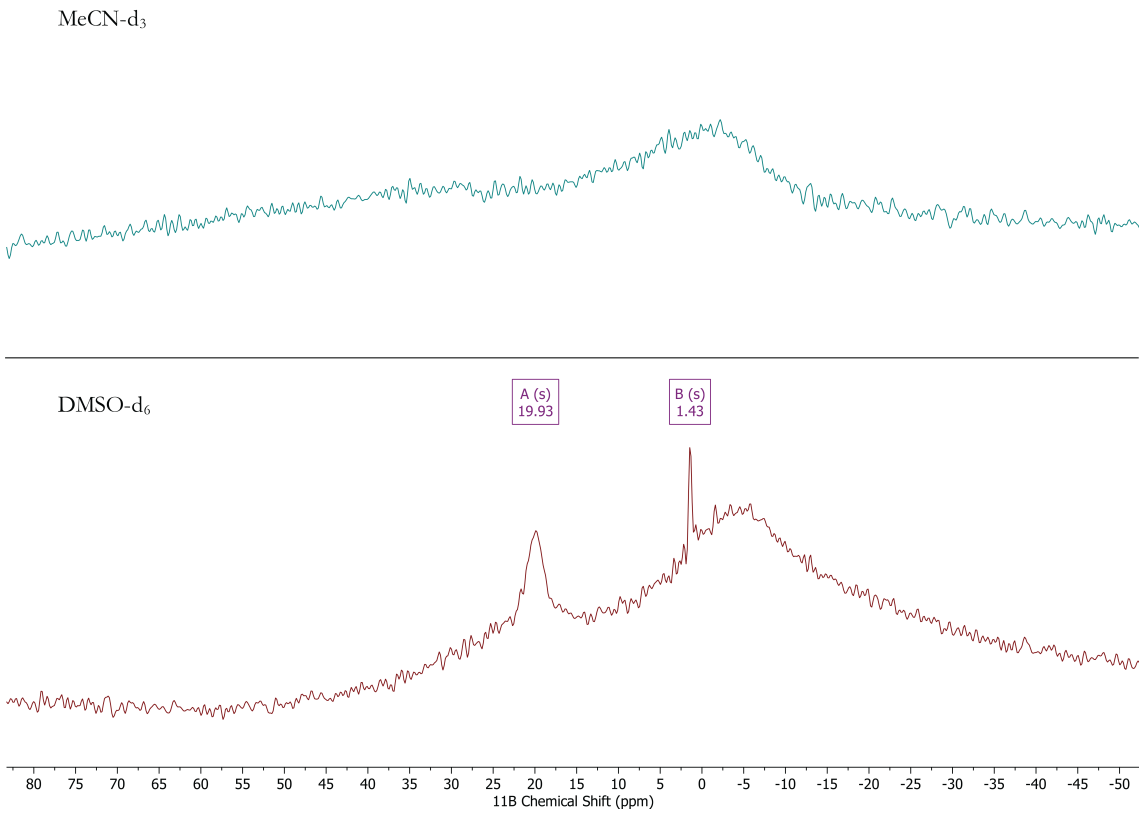

Figure 2-15: ^{11}B NMR (128 MHz, 25 °C) spectrum of the colorless solids isolated after photolysis of $^{i}Pr_2NBOA$ under an atmosphere of CO_2 in MeCN-d_3 (top) and DMSO-d_6 (bottom).

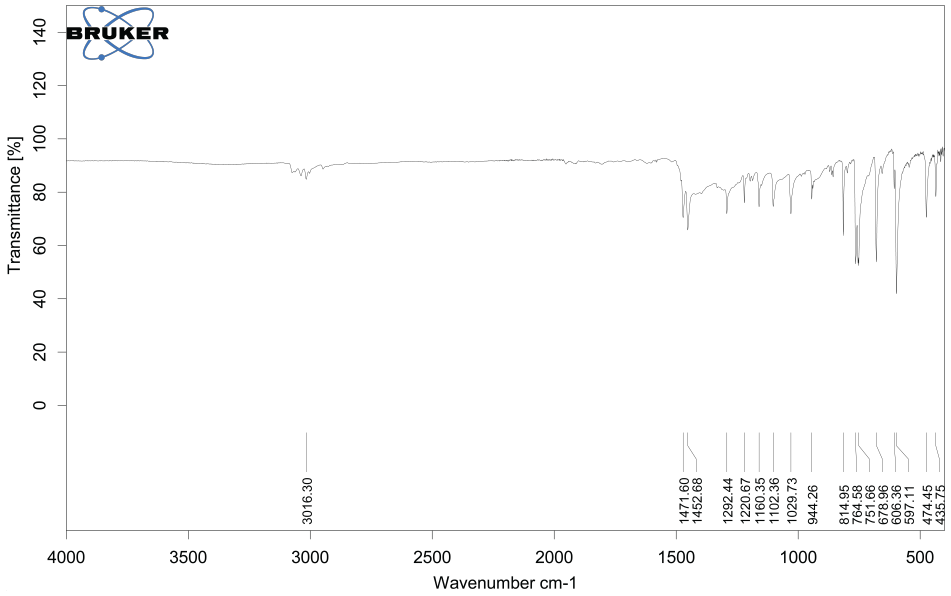

Figure 2-16: FT-IR spectrum of the colorless solids isolated after photolysis of $^{i}Pr_2NBOA$ under an atmosphere of CO_2.

Hydrolysis of putative $(^{i}Pr_2NBO)_2(CO_2)$

The solids isolated from the experiment described above were transferred to an NMR tube then removed from the glovebox. Deuterium oxide (0.7 mL) was added to the tube, which was subsequently capped and agitated. A small amount of bubbling seemed to occur. Multinuclear NMR revealed a soluble boron species matching the chemical shift of boric acid (Fig. 2-17), and the proton spectrum confirmed the presence of free diisopropylamine (Fig. 2-18). A fraction of the material remained undissolved, which was later confirmed to be the anthracene photodimer.

2.3.7 Treatment of ClBA·Et_2O with PhIO

ClBA·Et_2O (30 mg, 0.101 mmol, 1.0 equiv) was weighed out in a small vial containing a stir bar, dissolved in DCM (1 mL), and cooled to -35 °C in the glovebox freezer. Solid polymeric PhIO (24 mg, 0.109 mmol, 1.08 equiv) was added to the cold solution, then the vial capped and placed on a stir plate in the freezer and allowed to stir in the dark for two days. The cold, slightly yellow reaction mixture was filtered through glass microfiber filter paper in a pipette into an NMR tube for analysis. Colorless

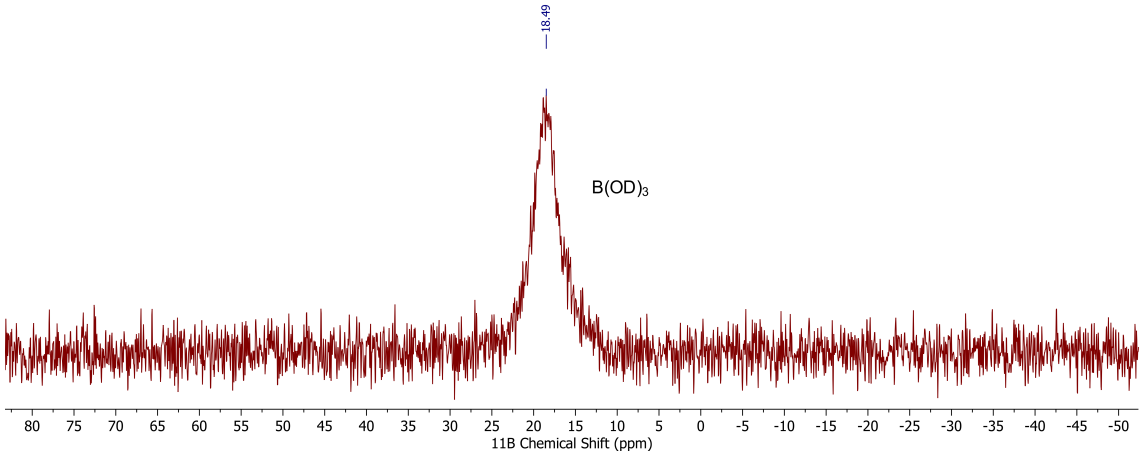

Figure 2-17: ^{11}B NMR (160 MHz, D_2O, 25 °C) spectrum of the colorless solids isolated from photolysis of $^{i}Pr_2$NBOA under an atmosphere of CO_2 after hydrolysis in D_2O.

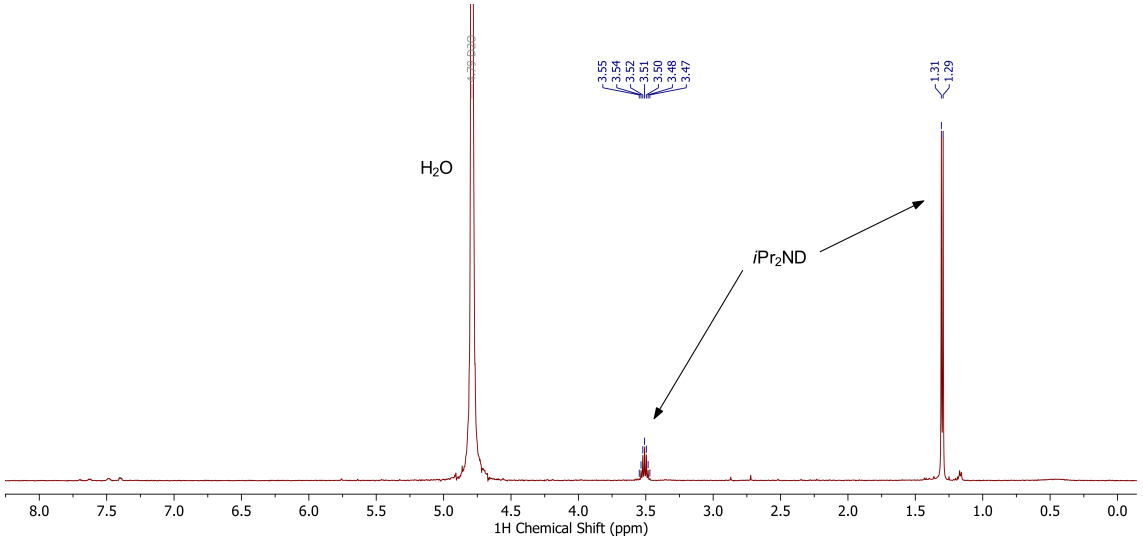

Figure 2-18: ^{1}H NMR (500 MHz, D_2O, 25 °C) spectrum of the colorless solids isolated from photolysis of $^{i}Pr_2$NBOA under an atmosphere of CO_2 after hydrolysis in D_2O.

solids began precipitating out of the filtered solution upon warming, which were later found to consist primarily of free anthracene according to proton NMR. The ^{11}B NMR spectrum displayed a broad ($\nu_{1/2}$ = 863 Hz) resonance at δ 37.2 ppm as the major species, along with a few convoluted smaller signals further upfield (Fig. 2-19).

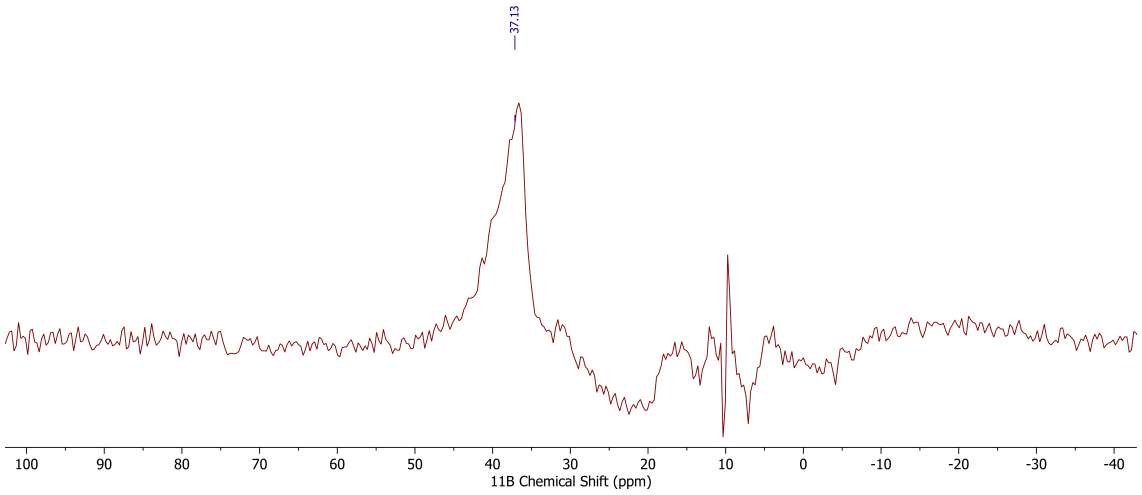

Figure 2-19: ^{11}B NMR (160 MHz, CH_2Cl_2, 25 °C) spectrum of the crude solution obtained after treatment of ClBA·Et_2O with PhIO at -35 °C.

2.4 X-Ray Diffraction Studies

Carried out with the assistance of Martin L. Y. Riu

Single crystals suitable for X-ray diffraction were transferred from the glovebox under Paratone oil onto a microscope slide. A crystal was selected under a microscope and mounted in hydrocarbon oil on a nylon loop. Low-temperature diffraction data were collected on a Bruker-AXS X8 Kappa Duo diffractometer with $I\mu S$ micro-sources, coupled to a Smart APEX2 CCD detector using Mo K_α radiation (λ = 0.71073 Å), performing ϕ- and ω-scans. The structures were solved by dual-space methods using SHELXT[51] and refined against F^2 on all data by full-matrix least squares with SHELXL-2017[51] following established refinement strategies.[52,53] All non-hydrogen atoms were refined anisotropically. All hydrogen atoms were included into the model at geometrically calculated positions and refined using a riding model. The isotropic displacement parameters of all hydrogen atoms were fixed to 1.2 times the U-value of the atoms they are linked to (1.5 times for methyl groups). Details of the data quality and a summary of the residual values of the refinement are listed in the table below.

Single crystals of ^{i}Pr$_2$NBOA were grown from diethyl ether at -35 °C. The structure was solved in the monoclinic space group $P2_1$ with two molecules of ^{i}Pr$_2$NBOA

and no solvent molecules in the asymmetric unit.

Table 2.1: Crystallographic Data for $^{i}Pr_2NBOA$

Identification code	P8_21115
Empirical formula, FW (g/mol)	$C_{20}H_{24}BNO$, 305.21
Color / Morphology	Colorless / Block
Crystal size (mm^3)	$0.240 \times 0.140 \times 0.100$
Temperature (K)	100(2)
Wavelength (Å)	0.71073
Crystal system, Space group	Monoclinic, $P2_1$
Unit cell dimensions (Å, °)	$a = 8.7108(3)$, $\alpha = 90.000$
	$b = 12.6046(5)$, $\beta = 95.8120(10)$
	$c = 15.8915(6)$, $\gamma = 90.000$
Volume ($Å^3$)	1735.86(11)
Z	4
Density (calc., g/cm^3)	1.168
Absorption coefficient (mm^{-1})	0.070
$F(000)$	656
Theta range for data collection (°)	1.288 to 31.543
Index ranges	$-12 \leq h \leq 12$, $-18 \leq k \leq 18$,
	$-23 \leq l \leq 22$
Reflections collected	117689
Independent reflections, R_{int}	11611, 0.0488
Completeness to $\theta_{\max}$ (%)	100.0
Absorption correction	Semi-empirical from equivalents
Refinement method	Full-matrix least-squares on F^2
Data / Restraints / Parameters	11611 / 1 / 423
Goodness-of-fit[a]	1.036
Final R indices[b] $[I > 2\sigma(I)]$	$R_1 = 0.0502$, $wR_2 = 0.1205$
R indices[b] (all data)	$R_1 = 0.0649$, $wR_2 = 0.1307$
Largest diff. peak and hole ($e \cdot Å^{-3}$)	0.477 and −0.256

[a] GooF $= \sqrt{\frac{\Sigma[w(F_o^2 - F_c^2)^2]}{(n-p)}}$ [b] $R_1 = \frac{\Sigma||F_o| - |F_c||}{\Sigma|F_o|}$; $wR_2 = \sqrt{\frac{\Sigma[w(F_o^2 - F_c^2)^2}{\Sigma[w(F_o^2)^2]}}$; $w = \frac{1}{\sigma^2(F_o^2) + (aP)^2 + bP}$; $P = \frac{2F_c^2 + \max(F_o^2, 0)}{3}$

2.5 Computational Details

2.5.1 Mechanism for fragmentation of $^{i}Pr_2NBOA$

All calculations were performed using the ORCA 5.0.0 quantum chemistry package.[54] Geometry optimizations and frequency calculations were performed at the `B3LYP-D3/def2-TZVP` level of theory using keywords `B3LYP D3BJ def2-TZVP def2/J TightSCF RIJCOSX Opt NumFreq`. The transition state geometry was determined using the Nudged Elastic Band (NEB) method, which was implemented using keyword `NEB-TS`. Intermediate and transition state geometries were found to have zero and one imaginary frequency, respectively. Electronic energies of the DFT-optimized geometries were calculated using the domain-based local pair natural orbital coupled-cluster method with singles, doubles, and perturbative triples excitation (DLPNO-CCSD(T))[55] with the cc-pVTZ basis set using keywords `cc-pVTZ cc-pVTZ/C DLPNO-CCSD(T1) TightSCF TightPNO`. DFT-calculated corrections for zero-point energy, thermal energy, and entropic effects were combined with the computed DLPNO-CCSD(T) electronic energies to obtain enthalpy, entropy, and free energy.[56]

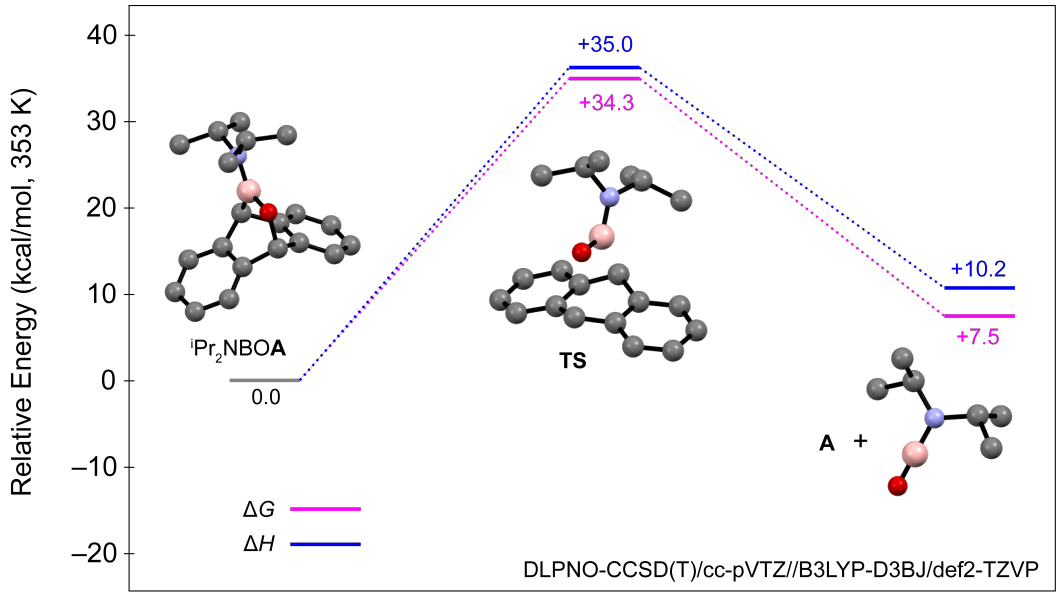

Figure 2-20: Calculated minimum energy pathway for $^{i}Pr_2NBOA$ fragmentation.

The above calculations were also repeated for a number of other potential RBOA molecules in order to assess the feasibility of their isolation, at least according to the unimolecular fragmentation pathway. Transition states for concerted elimination of anthracene and free RBO could be found using the NEB method in all cases, and results are tabulated below.

Compound	Calculated Barrier at 80 °C (kcal/mol)	Calculated ^{11}B Chemical Shift (ppm)
$^{i}Pr_2$NBOA	34.3	28.0
MeOBOA	36.3	30.5
HOBOA	33.9	30.6
HBOA	25.6	43.4
ClBOA	29.3	43.6
OTfBOA	31.3	32.4

Table 2.2: Predicted barriers to concerted elimination of RBO and A from several possible target molecules. Energy calculations were carried out at the DLPNO-CCSD(T)/cc-pVTZ level of theory and geometry optimizations and transition state searches at B3LYP-D3(BJ)/Def2-TZVP.

Bibliography

[1] Hillman, M. E. D. The Carbonylation of Organoboranes. III. The Reaction of Trialkylboranes with Carbon Monoxide and Aldehydes. Synthesis of a New Class of Organoboranes. *Journal of the American Chemical Society* **1963**, *85*, 1626–1628.

[2] Brown, H. C.; Pfaffenberger, C. D. Thexylborane as a convenient reagent for the cyclic hydroboration of dienes. Stereospecific syntheses via cyclic hydroboration. *Journal of the American Chemical Society* **1967**, *89*, 5475–5477.

[3] Borys, A. M.; Rice, E. F.; Nichol, G. S.; Cowley, M. J. The Phospha-Bora-Wittig Reaction. *Journal of the American Chemical Society* **2021**, *143*, 14065–14070.

[4] Kaiser, R. I.; Balucani, N. Exploring the Gas Phase Synthesis of the Elusive Class of Boronyls and the Mechanism of Boronyl Radical Reactions under Single Collision Conditions. *Accounts of Chemical Research* **2017**, *50*, 1154–1162.

[5] Bettinger, H. F. Reversible Formation of Organyl(oxo)boranes (RBO) (R = C $_6$ H $_5$ or CH $_3$) from Boroxins ((RBO) $_3$): A Matrix Isolation Study. *Organometallics* **2007**, *26*, 6263–6267.

[6] Bock, H.; Cederbaum, L.; Von Niessen, W.; Paetzold, P.; Rosmus, P.; Solouki, B. Methylboron Oxide, H3C?B?O. *Angewandte Chemie International Edition in English* **1989**, *28*, 88–90.

[7] Hildenbrand, D. L.; Theard, L. P.; Saul, A. M. Transpiration and Mass Spectrometric Studies of Equilibria Involving BOF(g) and (BOF) $_3$ (g). *The Journal of Chemical Physics* **1963**, *39*, 1973–1978.

[8] Deng, G.; Pan, S.; Jin, J.; Wang, G.; Zhao, L.; Zhou, M.; Frenking, G. Generation and Identification of the Linear OCBNO and OBNCO Molecules with 24 Valence Electrons. *Chemistry – A European Journal* **2021**, *27*, 412–418.

[9] Paetzold, P.; Neyses, S.; Gret, L. Oxo(trisyl)boran (Me3Si)3CBO als Zwischenstufe. *Zeitschrift fr anorganische und allgemeine Chemie* **1995**, *621*, 732–736.

[10] Lanzisera, D. V.; Andrews, L. Reactions of Laser-Ablated Boron Atoms with Methanol. Infrared Spectra and *ab Initio* Calculations of CH $_3$ BO, CH $_2$ BOH, and CH $_2$ BO in Solid Argon. *The Journal of Physical Chemistry A* **1997**, *101*, 1482–1487.

[11] Kawashima, Y.; Endo, Y.; Kawaguchi, K.; Hirota, E. Detection and equilibrium molecular structure of a short-lived molecule, HBO, by microwave spectroscopy. *Chemical Physics Letters* **1987**, *135*, 441–445.

[12] Ault, B. S. Excimer-laser-induced oxidation of diborane: Formation and isolation of HBO, HB18O AND H3B3O3 in argon matrices. *Chemical Physics Letters* **1989**, *157*, 547–551.

[13] Lory, E. R.; Porter, R. F. Infrared spectrum of matrix-isolated HBO. *Journal of the American Chemical Society* **1971**, *93*, 6301–6302.

[14] Kawashima, Y.; Kawaguchi, K.; Hirota, E. Detection of HBO by discharge modulated infrared diode laser spectroscopy. *Chemical Physics Letters* **1986**, *131*, 205–208.

[15] Kawashima, Y.; Endo, Y.; Hirota, E. Microwave spectrum, molecular structure, and force field of HBO. *Journal of Molecular Spectroscopy* **1989**, *133*, 116–127.

[16] Kawashima, Y.; Kawaguchi, K.; Endo, Y.; Hirota, E. Infrared diode laser and microwave spectra and molecular structure of an unstable molecule, FBO. *The Journal of Chemical Physics* **1987**, *87*, 2006–2009.

[17] Kawaguchi, K.; Endo, Y.; Hirota, E. Infrared diode laser and microwave spectroscopy of an unstable molecule: ClBO. *Journal of Molecular Spectroscopy* **1982**, *93*, 381–388.

[18] Pachaly, B.; West, R. Synthesis of a 1,3-dioxa-2,4-diboretane, an oxoborane precursor. *Journal of the American Chemical Society* **1985**, *107*, 2987–2988.

[19] Tokitoh, N.; Ito, M.; Okazaki, R. Formation and reactions of a thioxoborane, a novel boron-sulfur double-bond compound. *Tetrahedron Letters* **1996**, *37*, 5145–5148.

[20] Ito, M.; Tokitoh, N.; Okazaki, R. A novel approach to an oxoborane and its Lewis base complex. *Tetrahedron Letters* **1997**, *38*, 4451–4454.

[21] Ito, M.; Tokitoh, N.; Okazaki, R. 1,3,2,4-Diselenastannaboretane, a novel selenium-containing four-membered boracycle: synthesis, structure and thermal cycloreversion into a selenoxoborane. *Chemical Communications* **1998**, 2495–2496.

[22] Vidovic, D.; Moore, J. A.; Jones, J. N.; Cowley, A. H. Synthesis and Characterization of a Coordinated Oxoborane: Lewis Acid Stabilization of a BoronOxygen Double Bond. *Journal of the American Chemical Society* **2005**, *127*, 4566–4567.

[23] Bao, M.; Dai, Y.; Liu, C.; Su, Y. Acid/Base-Free Acyclic Anionic Oxoborane and Iminoborane Bearing Diboryl Groups. *Inorganic Chemistry* **2022**, *61*, 11137–11142.

[24] Loh, Y. K.; Porteous, K.; Fuentes, M. ; Do, D. C. H.; Hicks, J.; Aldridge, S. An Acid-Free Anionic Oxoborane Isoelectronic with Carbonyl: Facile Access and Transfer of a Terminal BO Double Bond. *Journal of the American Chemical Society* **2019**, *141*, 8073–8077.

[25] Nakano, R.; Yamanashi, R.; Yamashita, M. Base-Stabilized Neutral Oxoborane and Thioxoborane Supported by a Bis(oxazolinyl)(phenyl)methanide Ligand. *Chemistry – A European Journal* **2023**, *29*.

[26] Liu, R.; Gao, F.; Liu, J.; Wei, J.; Hou, L.; Xie, G.; Chen, S.; Zeng, F.; Li, A.; Wang, W. Anionic oxoborane and thioxoborane molecules supported by a 1,2-bis(imino)acenaphthene ligand. *Dalton Transactions* **2021**, *50*, 6797–6801.

[27] Franz, D.; Irran, E.; Inoue, S. Isolation of a Three-Coordinate Boron Cation with a Boron-Sulfur Double Bond. *Angewandte Chemie International Edition* **2014**, *53*, 14264–14268.

[28] Wang, H.; Zhang, J.; Hu, H.; Cui, C. Access to BS and BSe Double Bonds via Sulfur and Selenium Insertion into a BH Bond and Hydrogen Migration. *Journal of the American Chemical Society* **2010**, *132*, 10998–10999.

[29] Wang, Y.; Hu, H.; Zhang, J.; Cui, C. Comparison of Anionic and Lewis Acid Stabilized N-Heterocyclic Oxoboranes: Their Facile Synthesis from a Borinic Acid. *Angewandte Chemie International Edition* **2011**, *50*, 2816–2819.

[30] Liu, S.; Légaré, M.-A.; Auerhammer, D.; Hofmann, A.; Braunschweig, H. The First Boron-Tellurium Double Bond: Direct Insertion of Heavy Chalcogens into a Mn=B Double Bond. *Angewandte Chemie International Edition* **2017**, *56*, 15760–15763.

[31] Loh, Y. K.; Chong, C. C.; Ganguly, R.; Li, Y.; Vidovic, D.; Kinjo, R. 1,2,4,3-Triazaborole-based neutral oxoborane stabilized by a Lewis acid. *Chemical Communications* **2014**, *50*, 8561.

[32] Swarnakar, A. K.; Hering-Junghans, C.; Ferguson, M. J.; McDonald, R.; Rivard, E. Oxoborane (RBO) Complexation and Concomitant Electrophilic Bond Activation Processes. *Chemistry - A European Journal* **2017**, *23*, 8628–8631.

[33] Wang, H.; Zhang, J.; Yang, J.; Xie, Z. Synthesis, Structure, and Reactivity of Acid-Free Neutral Oxoborane. *Angewandte Chemie International Edition* **2021**, *60*, 19008–19012.

[34] Chen, P.; Cui, C. Isolable Boron Persulfide: Activation of Elemental Sulfur with a 2-Chloro-Azaborolyl Anion. *Chemistry - A European Journal* **2016**, *22*, 2902–2905.

[35] Stoy, A.; Härterich, M.; Dewhurst, R. D.; Jiménez-Halla, J. O. C.; Endres, P.; Eyßelein, M.; Kupfer, T.; Deissenberger, A.; Thiess, T.; Braunschweig, H. Evidence for Borylene Carbonyl (LHBCO) and Base-Stabilized (LHBO) and Base-Free Oxoborane (RBO) Intermediates in the Reactions of Diborenes with CO_2. *Journal of the American Chemical Society* **2022**, *144*, 3376–3380.

[36] Dolati, H.; Denker, L.; Trzaskowski, B.; Frank, R. Superseding beta-Diketiminato Ligands: An Amido Imidazoline-2-Imine Ligand Stabilizes the Exhaustive Series of B=X Boranes (X=O, S, Se, Te). *Angewandte Chemie International Edition* **2021**, *60*, 4633–4639.

[37] Braunschweig, H.; Radacki, K.; Schneider, A. Oxoboryl Complexes: Boron Oxygen Triple Bonds Stabilized in the Coordination Sphere of Platinum. *Science* **2010**, *328*, 345–347.

[38] Soderquist, J. A.; Najafi, M. R. Selective oxidation of organoboranes with anhydrous trimethylamine N-oxide. *The Journal of Organic Chemistry* **1986**, *51*, 1330–1336.

[39] Tanaka, K.; Riu, M.-L. Y.; Valladares, B.; Cummins, C. C. Introducing *N* -Heterocyclic Iminophosphoranes (NHIPs): Synthesis by [3 + 2] Cycloaddition of Azophosphines with Alkynes and Reactivity Studies. *Inorganic Chemistry* **2022**, *61*, 13662–13666.

[40] Pyykkö, P. Additive Covalent Radii for Single-, Double-, and Triple-Bonded Molecules and Tetrahedrally Bonded Crystals: A Summary. *The Journal of Physical Chemistry A* **2015**, *119*, 2326–2337.

[41] Larkin, J. D.; Bhat, K. L.; Markham, G. D.; James, T. D.; Brooks, B. R.; Bock, C. W. A Computational Characterization of BoronOxygen Multiple Bonding in HNCHCHCHNHBO. *The Journal of Physical Chemistry A* **2008**, *112*, 8446–8454.

[42] Greenfield, H.; Sternberg, H. W.; Friedel, R. A.; Wotiz, J. H.; Markby, R.; Wender, I. Acetylenic Dicobalt Hexacarbonyls. Organometallic Compounds Derived from Alkynes and Dicobalt Octacarbonyl [1,2]. *Journal of the American Chemical Society* **1956**, *78*, 120–124.

[43] Jutzi, P.; Möhrke, A. Überraschende Reaktionen von Decamethylsilicocen mit -Systemen des Typs X=C=Y. *Angewandte Chemie* **1989**, *101*, 769–770.

[44] Knowles, D. J.; Buchanan, A. S. The Preparation and Thermal Stability of Trichloroboroxine. *Inorganic Chemistry* **1965**, *4*, 1799–1802.

[45] Pangborn, A. B.; Giardello, M. A.; Grubbs, R. H.; Rosen, R. K.; Timmers, F. J. Safe and Convenient Procedure for Solvent Purification. *Organometallics* **1996**, *15*, 1518–1520.

[46] Williams, D. B. G.; Lawton, M. Drying of Organic Solvents: Quantitative Evaluation of the Efficiency of Several Desiccants. *The Journal of Organic Chemistry* **2010**, *75*, 8351–8354.

[47] Altintas, O.; Glassner, M.; Rodriguez-Emmenegger, C.; Welle, A.; Trouillet, V.; Barner-Kowollik, C. Macromolecular Surface Design: Photopatterning of Functional Stable Nitrile Oxides. *Angewandte Chemie International Edition* **2015**, *54*, 5777–5783.

[48] Plotkin, J. S.; Shore, S. G. Convenient preparation and isolation of pure potassium cyclopentadienyldicarbonylferrate, K[(.eta.5-C5H5)Fe(CO)2]. *Inorganic Chemistry* **1981**, *20*, 284–285.

[49] Fulmer, G. R.; Miller, A. J. M.; Sherden, N. H.; Gottlieb, H. E.; Nudelman, A.; Stoltz, B. M.; Bercaw, J. E.; Goldberg, K. I. NMR Chemical Shifts of Trace Impurities: Common Laboratory Solvents, Organics, and Gases in Deuterated Solvents Relevant to the Organometallic Chemist. *Organometallics* **2010**, *29*, 2176–2179.

[50] Pauson, P. L.; Stambuli, J. P.; Chou, T.-C.; Hong, B.-C. *Encyclopedia of Reagents for Organic Synthesis*; John Wiley & Sons, Ltd: Chichester, UK, 2014; pp 1–26.

[51] Sheldrick, G. M. SHELXT – Integrated space-group and crystal-structure determination. *Acta Crystallographica Section A Foundations and Advances* **2015**, *71*, 3–8.

[52] Müller, P.; Herbst-Irmer, R.; Spek, A. L.; Schneider, T. R.; Sawaya, M. R. *Crystal Structure Refinement*; Oxford University Press, 2006.

[53] Müller, P. Practical suggestions for better crystal structures. *Crystallography Reviews* **2009**, *15*, 57–83.

[54] Neese, F. Software update: The ORCA program system—Version 5.0. *WIREs Computational Molecular Science* **2022**, *12*.

[55] Guo, Y.; Riplinger, C.; Becker, U.; Liakos, D. G.; Minenkov, Y.; Cavallo, L.; Neese, F. Communication: An improved linear scaling perturbative triples correction for the domain based local pair-natural orbital based singles and doubles coupled cluster method [DLPNO-CCSD(T)]. *The Journal of Chemical Physics* **2018**, *148*, 011101.

[56] Paulechka, E.; Kazakov, A. Efficient DLPNO–CCSD(T)-Based Estimation of Formation Enthalpies for C-, H-, O-, and N-Containing Closed-Shell Compounds Validated Against Critically Evaluated Experimental Data. *The Journal of Physical Chemistry A* **2017**, *121*, 4379–4387.

Chapter 3

Progress Towards the Generation of Boron-Pnictogen Multiply Bonded Species

3.1 Introduction

The synthesis and isolation of molecules featuring boron-pnictogen multiple bonds has been of substantial interest for decades and continues to be a large research topic due to the attractive chemical and physical properties of materials containing functionalities that are isoelectronic to unsaturated carbon-carbon bonds, yet highly polarized. Iminoboranes (RBNR) have been quite well studied since the 1980s by Paetzold and coworkers, and are readily prepared via the thermolysis of azidoboranes, among other methods.[1] Since then, interest has grown in synthesizing their heavier analogues, boraphosphenes (RBPR). This goal is made fundamentally difficult due to the poor pπ overlap of group 13 and 15 elements, and others have relied principally on the use of highly sterically demanding substituents to coerce boron and phosphorus into forming π-bonds. Using this strategy, and/or employing strong donors or acceptors, Cowley, Noth, Power, Andrada, and Gilliard have all isolated and characterized molecules containing boron-phosphorus double bonds.[2–9] More re-

cently, Liu and coworkers have demonstrated the preparation of the first isolable free phosphaborene that is stable against oligomerization via the use of a powerful π-donor/π-acceptor push-pull framework with N-heterocyclic imine and N-heterocyclic boryl ligands.[10] Finally, not long before the time of writing, Manners and coworkers reported the isolation of a phosphaborene with the shortest BP bond distance thus far of 1.741(3) Å, slightly shorter than the sum of double bond covalent radii.[11,12] Nonetheless, the reactivity of species containing a BP triple bond remains entirely unexplored due to synthetic difficulties. Thus, we aimed to prepare anthracene-based precursors that would allow for the generation and/or transfer of species containing boron-pnictogen multiple bonds, potentially with lower coordination numbers than previously feasible.

3.2 Synthesis and Preliminary Reactivity of ^{Et}CAAC·ABPCO

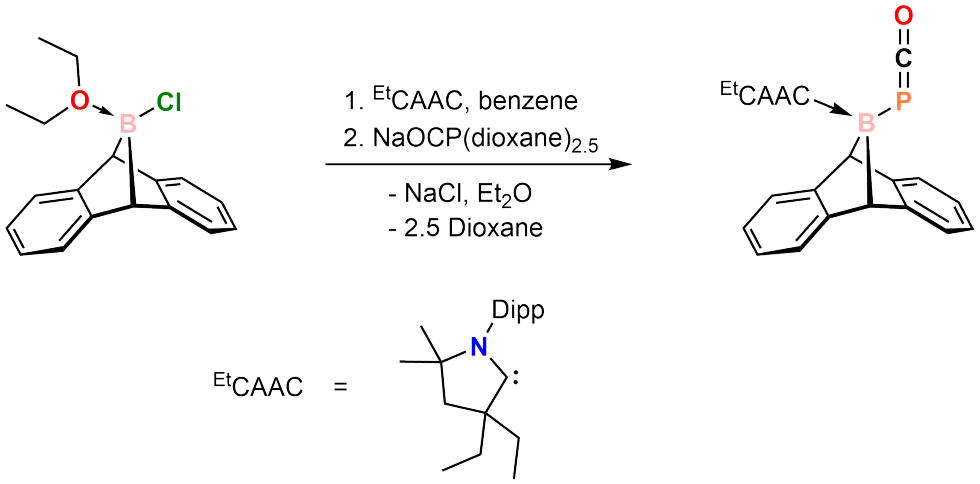

Figure 3-1: Synthesis of ^{Et}CAAC·ABPCO from ClBA·Et_2O by salt elimination.

In order to craft a molecular precursor suitable for the generation of a highly unstable intermediate, it is desirable to have thermodynamically favorable gas evolution occur in addition to anthracene elimination and rearomatization. With this in mind, we sought to synthesize an anthracene-based boraphosphaketene, containing a

B-PCO moiety that might decarbonylate and lead to the formation of interesting low-coordinate species. Although direct treatment of ClBA·THF in THF solution with Na(OCP)·2.5(dioxane) led only to the loss of ^{31}P NMR signal without formation of the desired product, addition of the phosphaethynolate salt to a benzene solution of the cyclic(alkyl)(amino)carbene (CAAC) adduct ^{Et}CAAC·ClBA led to successful NaCl elimination with selective formation of a new compound with an ^{11}B NMR chemical shift of δ 7.2 ppm and ^{31}P δ -286.9 ppm. The outcome of such reactions has been previously debated, given the highly oxophilic nature of boron, however it has been established that the phosphaketene isomer is likely to form over the phosphaethynolate.[13] Although a solid-state structure has not yet been obtained due to limited availability of reagents, the identity of the isolated compound as the boraphosphaketene ^{Et}CAAC·ABPCO has been confirmed by both IR spectroscopy, displaying a strong PCO stretching frequency at 1916 cm^{-1}, and the boron isotope effect in the ^{31}P NMR spectrum, where two signals integrating in a 4:1 ratio are observed at approximately the same chemical shift and correspond to ^{11}B - ^{31}P and ^{10}B - ^{31}P linkages, respectively.

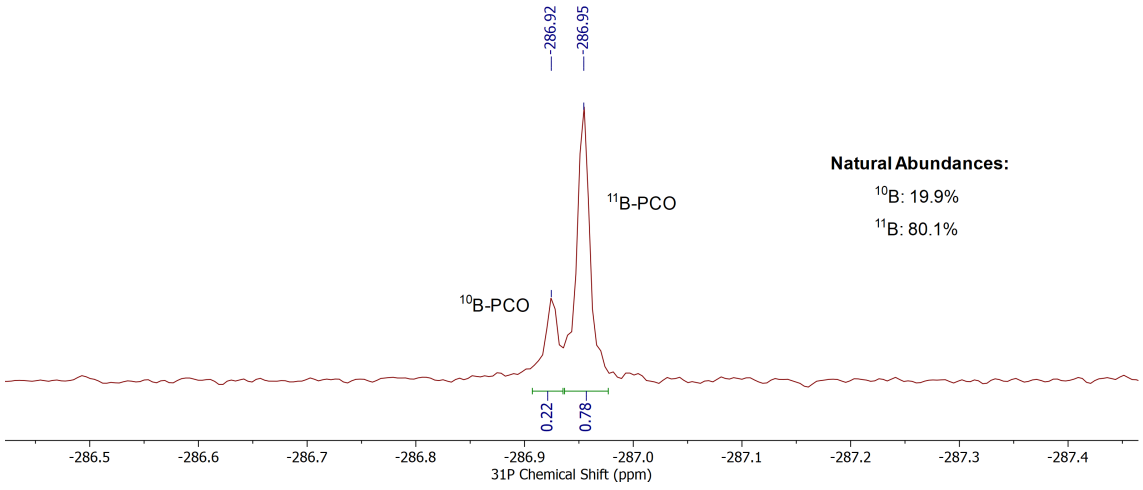

Figure 3-2: ^{31}P NMR (202 MHz, Benzene-*d*6, 25 °C) spectrum of ^{Et}CAAC·ABPCO exhibiting the boron isotope effect, thus confirming boron-phosphorus connectivity.

Only a small set of other boraphosphaketenes have been described in the literature by Goicoechea, Gilliard, and Braunschweig,[9,13,14] hence much of the chemistry of these

compounds is not well understood. However, it is known that they are generally stable to thermolysis and decarbonylation must instead be effected by UV photolysis. Photolysis of a benzene solution of ^{Et}CAAC·ABPCO with 254 nm light led to a striking color change from orange to deep purple, although the analysis of the products has been limited. Interestingly, although multiple new boron-containing species could be observed in the ^{11}B NMR spectrum, only a single signal was observed via ^{31}P NMR at δ -29.2 ppm with poor signal to noise. The decarbonylation chemistry of Goicoechea's group 13 phosphaketenes has been described to be similar, but heavily dependent on the properties of the Lewis base bound to boron. They eventually isolated diphosphenes as the product of photolysis, however ^{31}P solution state NMR could not be collected and EPR spectroscopy indicated the presence of unidentifiable radical species in solution. It is expected that the fate of ^{Et}CAAC·ABPCO may be very similar, though further work is needed to confirm this.

We further attempted to photolytically decarbonylate our boraphosphaketene in the presence of a chemical trap, dicyclohexyl ketone. Interested to see if any of the anthracene-eliminated low-valent species, ^{Et}CAAC·BP, was formed under these conditions, this particular substrate was chosen to allow for favorable B-O bond formation. A single new ^{11}B NMR resonance was observed at δ 8.8 ppm, likely corresponding to a tetracoordinate boron species given its upfield chemical shift and relatively sharp peak ($\nu_{1/2}$ = 52.9 Hz). Although very messy, ^{1}H NMR did not indicate the presence of free anthracene, thus the identity of this product was putatively assigned as an oxaphosphirane formed by addition of the transient boraphosphinidene to the ketone. Interestingly, however, similar issues as described above were encountered in the ^{31}P NMR analysis and the dominant species was residual ^{Et}CAAC·ABPCO rather than a corresponding new signal. The cause of this discrepancy is currently unknown.

Given the challenges associated with photochemistry, we were also interested in studying options for chemical decarbonylation. Upon addition of a slight excess of *tert*-butyl isocyanide to a benzene solution of ^{Et}CAAC·ABPCO, clean and complete conversion to a new species exhibiting a sharp ^{11}B NMR signal at δ 0.60 ppm, assigned as the base-stabilized boraphosphinidene ^{Et}CAAC·ABP(CN^{t}Bu), was observed. This

type of reaction has been well-described in prior literature and is known to occur readily in the case of other boraphosphaketenes.[14] Still, a corresponding ^{31}P NMR signal could not be observed. Given the very small scale ($\sim$ 10 mg) of the attempted reactions, it is possible to imagine that the low-coordinate phosphorus experiences significant peak-broadening due to the magnetic effects of adjacent boron, and further studies are needed to both confirm the outcome of this reaction and attempt to determine the cause of the unexpected ^{31}P NMR complications described here.

3.3 Reactivity of $(N_3BA)_3$

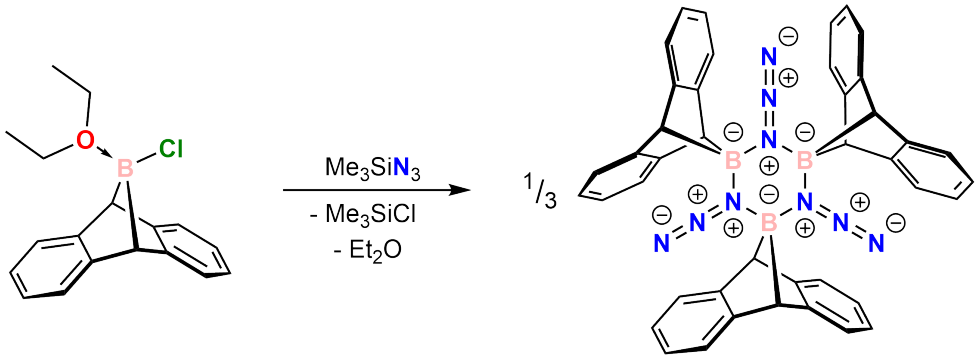

Figure 3-3: Synthesis of $(N_3BA)_3$ from ClBA·Et_2O via TMSCl elimination. Developed by André Eckhardt.

As a simple route towards opening up a new route to low-valent boron-nitrogen chemistry, postdoctoral researcher André Eckhardt developed the synthesis of N_3BA via the simple treatment of ClBA·Et_2O with $TMSN_3$. Its relatively high-field ^{11}B NMR resonance of δ 9.1 ppm, along with a single crystal x-ray diffraction study, indicated that this compound exists as a cyclotrimer in the solid-state and when dissolved in non-coordinating solvents. It is relatively easily broken up and readily forms one-to-one complexes upon addition of strong Lewis bases such as phosphines and N-heterocyclic carbenes. A mixture of $(N_3BA)_3$ and one-to-one adduct may be observed in the case of weaker Lewis bases, such as tetrahydrofuran, with reformation of the trimer upon evaporation of the solvent under reduced pressure.

Initially inspired by Rivard and coworker's successful stabilization of the parent

iminoborane within a frustrated Lewis pair,[15] we attempted to adapt this method for the stabilization of molecular boron mononitride. Unfortunately, it was found that the steric demands of the NHCs available to us (IMes, IPr), which would also provide stability against oligomerization, along with those of the anthracene moiety, inhibited binding of suitable Lewis bases such as BAr^F_3 to the alpha nitrogen lone pair. Moreover, although $(N_3BA)_3$ readily decomposes with N_2 evolution upon heating to only 42 °C, the adduct IPr·N_3BA showed no signs of decomposition upon heating to 80 °C for several days (work primarily by André Eckhardt).

Informed by the above results, focus was shifted towards a related goal: the preparation of a BN metal complex. Although a number of σ-iminoboryl complexes, L_nMBNR, have been described in the literature,[16] BN complexes have not yet been successfully synthesized, to the best of our knowledge. We first studied the interaction of $(N_3BA)_3$ with the nucleophilic cyclopentadienyliron dicarbonyl anion in the form of FpK. Although it offers little in the way of steric protection, the ease of availability of this particular complex and potential for π-backbonding promoted by a negative charge were attractive features. Addition of stoichiometric FpK to a thawing solution of $(N_3BA)_3$ in THF led to the selective formation of a new deep red species exhibiting an ^{11}B NMR resonance at δ 12.1 ppm. Based on the relatively sharp nature of this signal ($\nu_{1/2}$ = 46.6 Hz), along with the absence of free anthracene according to proton NMR, this new compound was identified as the metalate $[K(THF)_x][Fp(N_3BA)]$ in which a molecule of N_3BA binds as a Z-ligand to the iron center. In stark contrast to its NHC adducts, this complex was found to be quite thermally sensitive, and the formation of free anthracene can be observed via NMR upon heating to temperatures as low as 45 °C. No new signals could be observed via ^{11}B NMR, however.

The next logical step was to investigate the interaction of K[Fp(N_3BA)] with a strong Lewis base. A fresh solution of $[K(THF)_x][Fp(N_3BA)]$ was prepared, the solvent evaporated, and the material solvated in toluene with the aid of 18-crown-6. Addition of $B(C_6F_5)_3$ to this solution did not lead to much of a visible change, however ^{11}B NMR analysis revealed the complete consumption of BCF and near-complete consumption of $[K(18\text{-c-}6)(THF)_x][Fp(N_3BA)]$. Two dominant new species

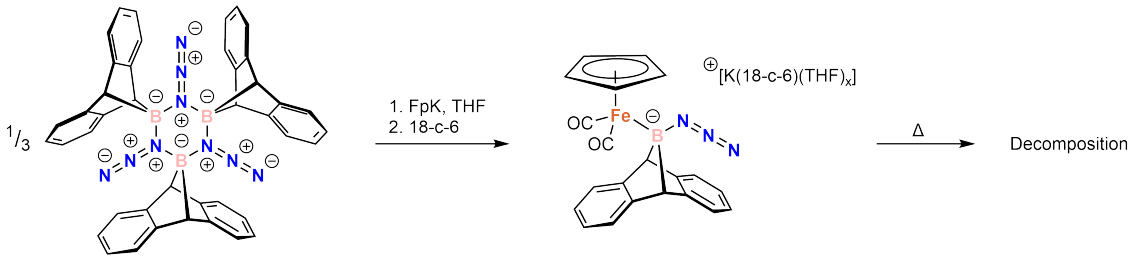

Figure 3-4: Ring opening of the $(N_3BA)_3$ cyclotrimer via addition of FpK with formation of a new iron azidoborane complex.

were observed with ^{11}B chemical shifts of δ 30.1 and 2.4 ppm, with the former being extremely broad; the fitted Lorentzian had a half-maximum width of approximately 2500 Hz. Given its chemical shift value, far enough from the typical location of ^{11}B background, and that the baseline was otherwise relatively flat due to probe background suppression with a phase cycled composite pulse,[17] this indeed appeared to be an interesting new signal. Isolable boron compounds exhibiting such broad resonances in solution are rare, with two well-known examples being Braunschweig's platinum oxoboryl complex ($\nu_{1/2}$ = 2111 Hz) and Figueroa's iron boron monofluoride complex ($\nu_{1/2}$ = 1820 Hz).[18,19] Based on the two-coordinate nature of boron in these reported complexes, I have proposed that an iron BN complex capped by BCF might be formed in the experiment described here. An ^{11}B - ^{11}B gCOSY experiment was carried out in an attempt to correlate the observed signals, however their extremely broad nature made this impossible. Further work verifying the reproducibility of this result and aiming to properly characterize this new species is currently ongoing as of the time of writing.

3.4 Experimental Details

3.4.1 General Information

Except as otherwise noted, all manipulations were performed in a Vacuum Atmospheres model MO-40M glovebox under an inert atmosphere of purified N_2. All solvents were obtained anhydrous and oxygen-free by bubble degassing (Ar), pas-

sage through columns of alumina using a solvent purification system (Pure Process Technology, Nashua, NH),[20] and storage over 4.0 Å molecular sieves.[21] Deuterated solvents were purchased from Cambridge Isotope Labs and degassed by three freeze-pump-thaw cycles and stored over 4 Å molecular sieves for at least 48 h prior to use. Diatomaceous earth (EM Science) and 4 Å molecular sieves were dried by heating above 200 °C under dynamic vacuum for at least 48 h prior to use. All glassware was dried in an oven for at least two hours at temperatures greater than 150 °C.

^{Et}CAAC,[22] NaOCP·2.5(dioxane),[23] FpK,[24] and tris(pentafluorophenyl)borane[25] were prepared according to literature procedures. Dicyclohexyl ketone (TCI Chemicals) and *tert*-butyl isocyanide (Sigma-Aldrich) were degassed by three freeze-pump-thaw cycles and stored over 4 Å molecular sieves prior to use. Azidotrimethylsilane (Sigma-Aldrich) and 18-crown-6 (Sigma-Aldrich) were used as received.

NMR spectra were obtained on a Bruker Avance 400 instrument equipped with a Magnex Scientific or with a SpectroSpin superconducting magnet or on a Bruker Avance 500 instrument equipped with a Magnex Scientific or with a SpectroSpin superconducting magnet. ^{1}H and ^{13}C NMR spectra were referenced internally to residual solvent signals.[26] ^{11}B and ^{31}P NMR spectra were externally referenced to 15% $BF_3{\cdot}Et_2O$ in $CDCl_3$ (0 ppm) and 85% H_3PO_4 (0 ppm), respectively.

Photochemical reactions were performed using a Rayonet photochemical reactor RPR-200 (Southern New England Ultra Violet Company) loaded with 16 RPR-2537A lamps, each emitting ca. 35 W at 253.7 nm.

3.4.2 Synthesis of ^{Et}CAAC·ABPCO

Solid ClBA·THF (150 mg, 0.534 mmol, 1.0 equiv) was weighed out in a scintillation vial and suspended in toluene (12 mL). Solid ^{Et}CAAC (166 mg, 0.530 mmol, 0.99 equiv) was added portionwise to the solution and the resulting nearly homogeneous mixture stirred for 15 minutes. With vigorous stirring, solid NaOCP·2.5(dioxane) (160 mg, 0.530 mmol, 0.99 equiv) was added in small portions over the course of five minutes. The vial was capped and protected from light with aluminum foil, and the heterogeneous reaction mixture stirred for 16 hours at ambient temperature.

The resulting brown slurry was filtered through a medium sintered frit containing a small plug of celite and charcoal. The vial and frit were washed with 20 mL additional toluene and the combined filtrates evaporated under reduced pressure, yielding ^{Et}CAAC·ABPCO as a bright orange powder (153mg, 0.280 mmol, 53%). ^{11}B NMR (Benzene-d_6, 160 MHz, 25 °C) δ 7.2 ppm. ^{31}P NMR (Benzene-d_6, 202 MHz, 25 °C) δ -286.9 ppm.

Infrared spectrum of ^{Et}CAAC·ABPCO

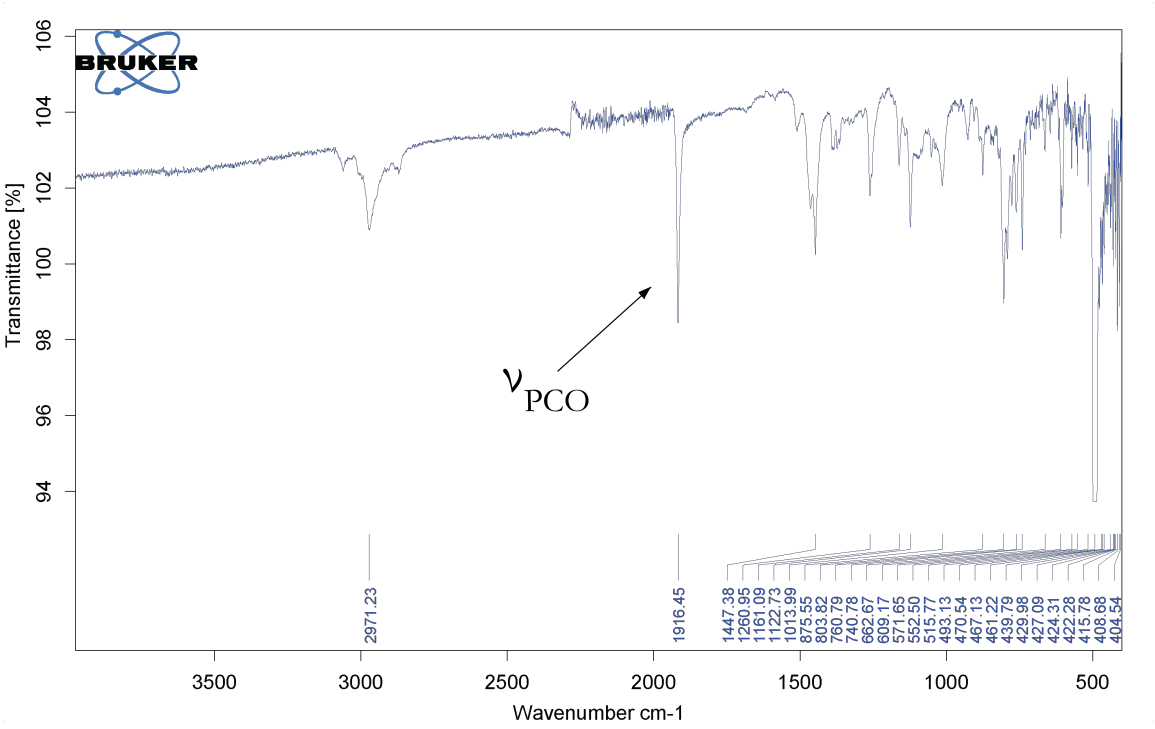

Figure 3-5: ^{11}B NMR spectrum (128 MHz, THF-H, 25 °C) of a solution of $(N_3BA)_3$ after low-temperature addition of FpK. Clean conversion to the adduct K[Fp(N_3BA)] is observed.

Photolysis of ^{Et}CAAC·ABPCO

Solid orange ^{Et}CAAC·ABPCO (11 mg, 0.020 mmol) was transerred to a J Young tube along with deuterated benzene (0.7 mL). The tube was capped and shaken vigorously to fully dissolve the material. The sample was removed from the glovebox and placed

in a Rayonet photoreactor equipped with a 254 nm bulb. Exposure over the course of three hours led to a color change first to dark red then deep purple, by which point NMR analysis indicated the complete consumption of starting material. Three major boron species were observable at ^{11}B δ 30.8, 3.4, and -7.5 ppm, however they were not easily separable at this scale.

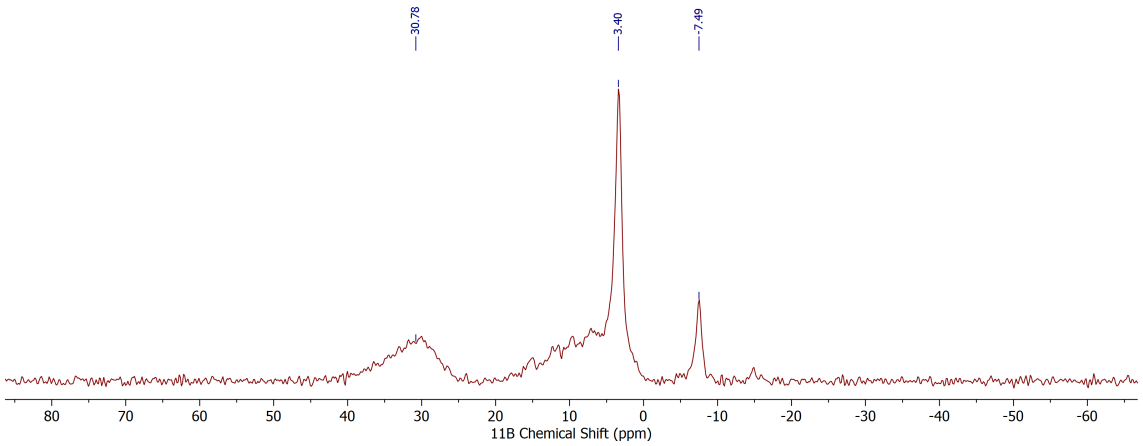

Figure 3-6: ^{11}B NMR spectrum (160 MHz, Benzene-d_6, 25 °C) of $^{\text{Et}}$CAAC·ABPCO after photolysis in the absence of a trap.

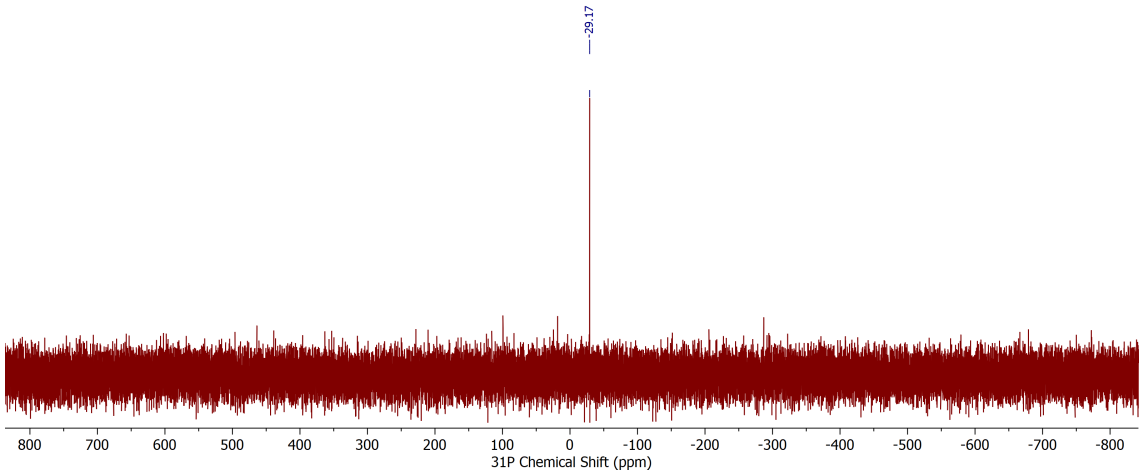

Figure 3-7: ^{31}P NMR spectrum (202 MHz, Benzene-d_6, 25 °C) of $^{\text{Et}}$CAAC·ABPCO after photolysis in the absence of a trap.

Photolysis of ^{Et}CAAC·ABPCO with Cy_2CO

^{Et}CAAC·ABPCO (10 mg, 0.0184 mmol, 1.0 equiv), Cy_2CO (36 mg, 0.186 mmol, 10 equiv), and deuterated benzene (1 mL) were combined in a small vial with stirring. The homogeneous orange solution was transferred to a J Young tube, sealed, then removed from the glovebox and placed in a Rayonet photoreactor equipped with a 254 nm bulb. After 25 minutes, ^{11}B NMR indicated near-complete conversion to a new species resonating at δ 8.8 ppm. A corresponding ^{31}P signal could not be identified.

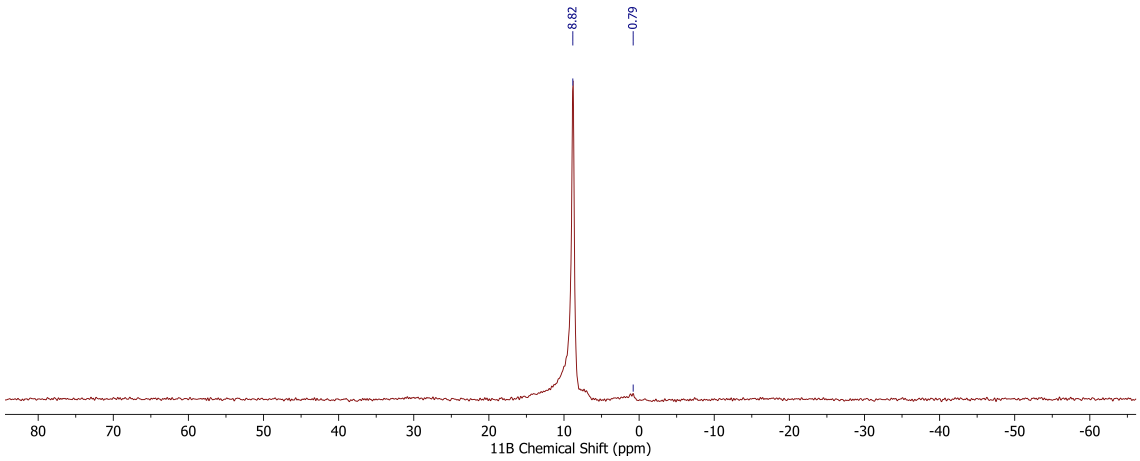

Figure 3-8: ^{11}B NMR spectrum (128 MHz, Benzene-d_6, 25 °C) of a solution of ^{Et}CAAC·ABPCO after photolysis in the presence of excess dicyclohexyl ketone.

Treatment of ^{Et}CAAC·ABPCO with ^{t}BuNC

Solid ^{Et}CAAC·ABPCO (10 mg, 0.0184 mmol, 1.0 equiv) was weighed out in a small vial and solvated in deuterated benzene (0.7 mL). An excess of ^{t}BuNC (one drop) was added via pipette, and the reaction mixture stirred for 16 hours. The homogeneous orange solution was transferred to an NMR tube for analysis. Complete conversion to a new species at ^{11}B δ 0.60 ppm was observed, however a corresponding ^{31}P NMR signal was not visible.

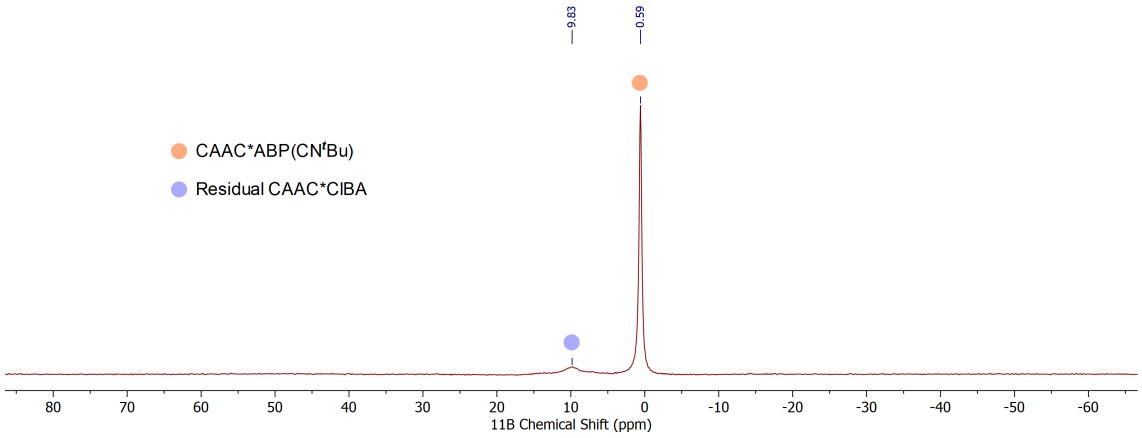

Figure 3-9: ^{11}B NMR spectrum (128 MHz, Benzene-d_6, 25 °C) of a solution of ^{Et}CAAC·ABPCO after addition of ^{t}BuNC.

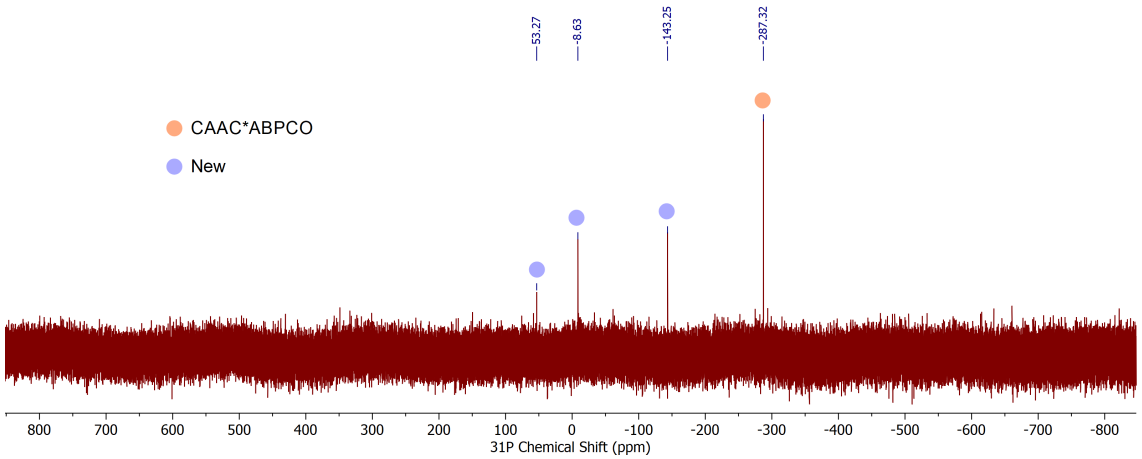

Figure 3-10: ^{31}P NMR spectrum (162 MHz, Benzene-d_6, 25 °C) of a solution of ^{Et}CAAC·ABPCO after addition of ^{t}BuNC

3.4.3 Synthesis of $(N_3BA)_3$

(Developed by André Eckhardt)

In the glovebox, a 20 mL scintillation vial was charged with solid ClBA·Et_2O (200 mg, 0.68 mmol, 1.0 equiv) and dichloromethane (4 mL). To the stirring solution was added $TMSN_3$ (85 mg, 0.74 mmol, 1.1 equiv) dropwise at room temperature and the reaction mixture was stirred for one hour, protected from light with aluminum foil, for an hour. All volatile material was removed under reduced pressure, then the residues were triturated with a small amount of pentane. The solids were carefully collected

and dried *in vacuo*, affording $(N_3BA)_3$ (141 mg, 90.5%) as a colorless solid. ^{1}H NMR (Benzene-d_6, 400 MHz, 25 °C) δ 7.08 (m, 12H), 6.86 (m, 12H), 3.18 (s, 6H) ppm. ^{11}B NMR (Benzene-d_6, 128 MHz, 25 °C) δ 9.1 (br s, $\nu_{1/2}$ = 397 Hz) ppm. ^{13}C{^{1}H} NMR (Benzene-d_6, 101 MHz, 25 °C) δ 148.0, 125.4, 123.3, 45.2 ppm.

Treatment of $(N_3BA)_3$ with FpK

Solid $(N_3BA)_3$ (50 mg, 0.072 mmol, 1.0 equiv) was carefully weighed out in a 20 mL scintillation vial and dissolved in THF (5 mL). The vial was placed in the glovebox coldwell until the solution was frozen. To the thawing solution with stirring was added solid orange FpK (47 mg, 0.217 mmol, 3.0 equiv) portionwise over the course of several minutes. The reaction vessel was capped, protected from light with aluminum foil, and allowed to warm to room temperature with stirring for an hour. An aliquot of the resulting very dark red solution was transferred to an NMR tube for spectroscopic analysis. ^{11}B NMR showed clean and complete conversion to a new species resonating at δ 12.1 ppm (relatively sharp, $\nu_{1/2}$ = 46.6 Hz), K[Fp(N_3BA)]. This compound has not yet been isolated in its pure solid form, but can be reliably prepared as a solution.

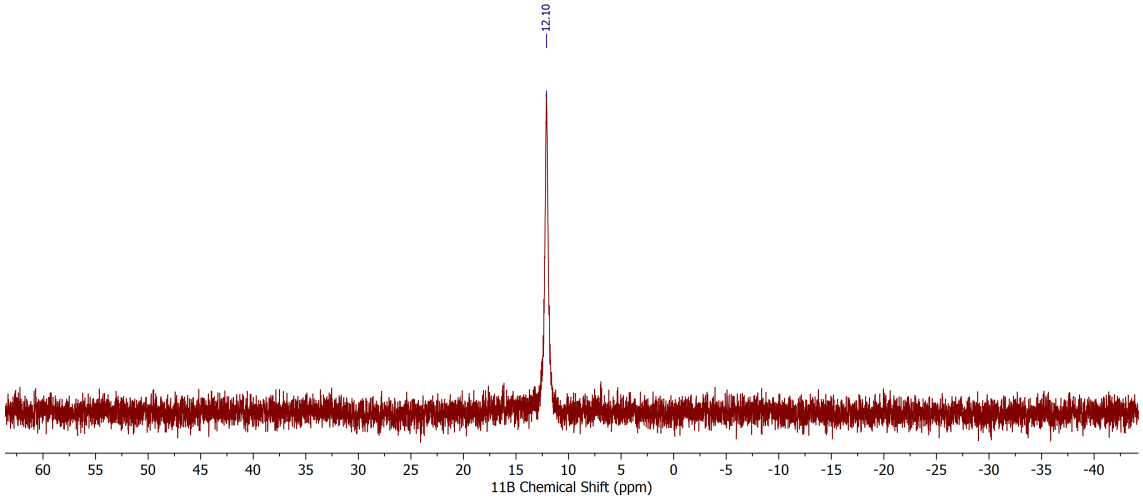

Figure 3-11: ^{11}B NMR spectrum (128 MHz, THF-H, 25 °C) of a solution of $(N_3BA)_3$ after low-temperature addition of FpK. Clean conversion to the complex K[Fp(N_3BA)] is observed.

Thermal stability of K[Fp(N_3BA)]

A sample (1 mL) of K[Fp(N_3BA)] solution in THF was transferred to a J Young tube. The tube was capped then placed in a 45 °C oil bath in the fumehood for 16 hours. The ^{1}H NMR signals were too broad to interpret entirely, however free anthracene could be easily identified in the solvent-suppressed spectrum, indicating that the compound had decomposed. No new resonances were detected by ^{11}B NMR.

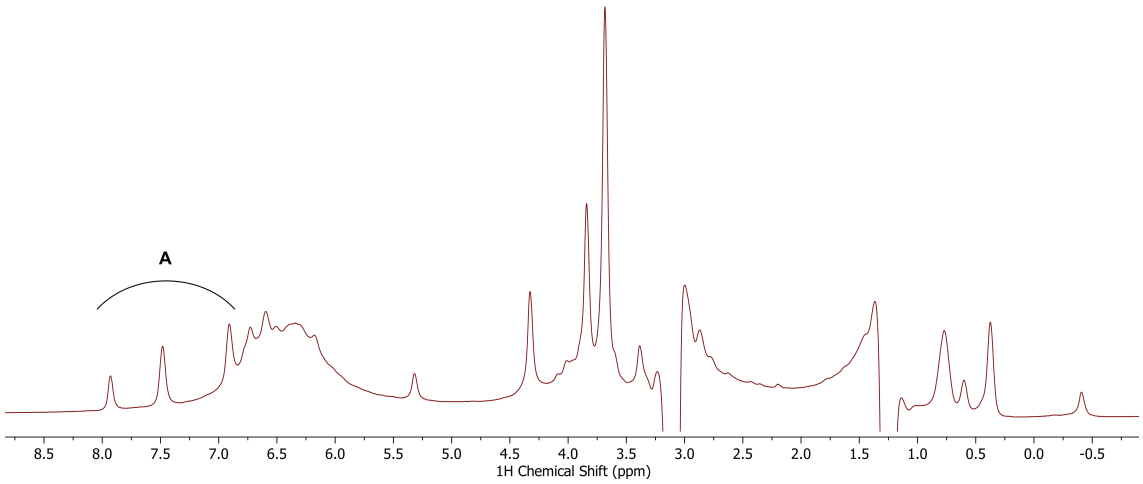

Figure 3-12: ^{1}H NMR spectrum (400 MHz, THF-H, 25 °C) of a solution of K[Fp(N_3BA)] after heating at 45 °C overnight. Although broad and improperly referenced, free anthracene signals are easily distinguishable and confirm that the compound decomposed.

Treatment of K[Fp(N_3BA)] with B(C_6F_5)$_3$

Solid (N_3BA)$_3$ (10 mg, 0.014 mmol, 0.33 equiv) was carefully weighed out in a 20 mL scintillation vial and dissolved in THF (1 mL). The vial was placed in the glove-box coldwell until the solution was frozen. To the thawing solution with stirring was added solid orange FpK (9.3 mg, 0.043 mmol, 1.0 equiv) in one portion. The reaction vessel was capped, protected from light with aluminum foil, and allowed to warm to room temperature with stirring. Solid 18-crown-6 (11.4 mg, 0.043 mmol, 1.0 equiv) was added and the mixture stirred for a further 10 minutes, then solvent was removed under reduced pressure. The residues were redissolved in toluene (1 mL) and

$B(C_6F_5)_3$ (22 mg, 0.043 mmol, 1.0 equiv) was added with strong stirring. The resulting nearly homogeneous solution was stirred for 30 minutes at room temperature, then transferred to a J Young tube for analysis. ^{11}B NMR revealed nearly complete consumption of K[Fp(N_3BA)] with the development of two new species resonating at δ 30.1 and 2.4 ppm, with the former being strikingly broad.

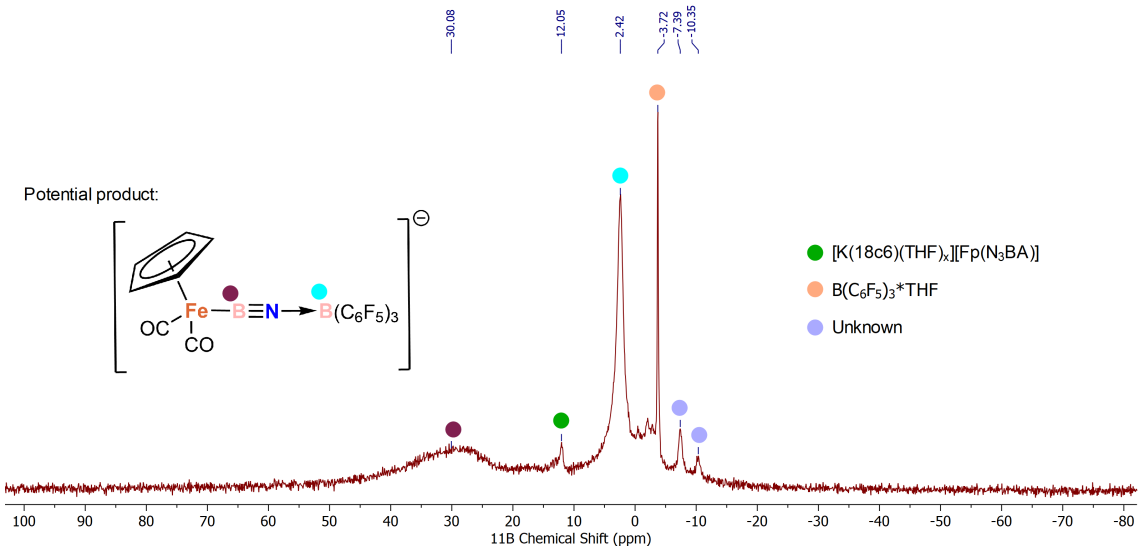

Figure 3-13: ^{11}B NMR spectrum (160 MHz, Toluene-H, 25 °C) of a solution of K[Fp(N_3BA] upon addition of BCF.

3.5 X-Ray Diffraction Studies

Carried out by André Eckhardt

Single crystals suitable for X-ray diffraction were transferred from the glovebox under Paratone oil onto a microscope slide. A crystal was selected under a microscope and mounted in hydrocarbon oil on a nylon loop. Low-temperature diffraction data were collected on a Bruker-AXS X8 Kappa Duo diffractometer with $I\mu S$ micro-sources, coupled to a Smart APEX2 CCD detector using Mo K_α radiation (λ = 0.71073 Å), performing ϕ- and ω-scans. The structures were solved by dual-space methods using SHELXT[27] and refined against F^2 on all data by full-matrix least squares with SHELXL-2017[27] following established refinement strategies.[28,29] All non-hydrogen

atoms were refined anisotropically. All hydrogen atoms were included into the model at geometrically calculated positions and refined using a riding model. The isotropic displacement parameters of all hydrogen atoms were fixed to 1.2 times the U-value of the atoms they are linked to (1.5 times for methyl groups). Details of the data quality and a summary of the residual values of the refinement are listed in the table below.

Single crystals of $(N_3BA)_3$ were grown from diethyl ether at -20 °C. The structure was solved in triclinic space group $P\bar{1}$, with two molecules of $(N_3BA)_3$ and two molecules of diethyl ether in the asymmetric unit. In one of the independent molecules of $(N_3BA)_3$, two of the azide moieties were refined as disordered over two positions.

Table 3.1: Crystallographic Data for $(N_3BA)_3$

Identification code	P8_21129
Empirical formula, FW (g/mol)	$C_{46.62}H_{38.97}B_3N_9O_{0.79}$, 770.35
Color / Morphology	Colorless / Plate
Crystal size (mm^3)	$0.300 \times 0.240 \times 0.020$
Temperature (K)	100(2)
Wavelength (Å)	0.71073
Crystal system, Space group	Triclinic, $P\bar{1}$
Unit cell dimensions (Å, °)	$a = 15.2446(13)$, $\alpha = 97.417(4)$
	$b = 16.5929(16)$, $\beta = 107.802(3)$
	$c = 17.2045(16)$, $\gamma = 95.440(3)$
Volume ($Å^3$)	4067.1(7)
Z	4
Density (calc., g/cm^3)	1.258
Absorption coefficient (mm^{-1})	0.077
$F(000)$	1612
Theta range for data collection (°)	1.250 to 30.508
Index ranges	$-21 \leq h \leq 21$, $-23 \leq k \leq 23$,
	$-24 \leq l \leq 24$
Reflections collected	239820
Independent reflections, R_{int}	24849, 0.0759
Completeness to $\theta_{\max}$ (%)	100.0
Absorption correction	Semi-empirical from equivalents
Refinement method	Full-matrix least-squares on F^2
Data / Restraints / Parameters	24849 / 1134 / 1277
Goodness-of-fit[a]	1.039
Final R indices[b] $[I > 2\sigma(I)]$	$R_1 = 0.0603$, $wR_2 = 0.1428$
R indices[b] (all data)	$R_1 = 0.0954$, $wR_2 = 0.1655$
Largest diff. peak and hole ($e \cdot Å^{-3}$)	0.425 and −0.536

[a] GooF $= \sqrt{\frac{\Sigma[w(F_o^2 - F_c^2)^2]}{(n-p)}}$ [b] $R_1 = \frac{\Sigma||F_o| - |F_c||}{\Sigma|F_o|}$; $wR_2 = \sqrt{\frac{\Sigma[w(F_o^2 - F_c^2)^2}{\Sigma[w(F_o^2)^2]}}$; $w = \frac{1}{\sigma^2(F_o^2) + (aP)^2 + bP}$; $P = \frac{2F_c^2 + \max(F_o^2, 0)}{3}$

3.6 Computational Details

3.6.1 UV/Vis Absorbance of ^{Et}CAAC·ABPCO

All calculations were performed using the ORCA 5.0.0 quantum chemistry package.[30] Geometry optimizations and frequency calculations were performed at the `B3LYP-D3/def2-TZVP` level of theory using keywords `B3LYP D3BJ def2-TZVP def2/J TightSCF RIJCOSX Opt NumFreq`. Given the poor accuracy of conventional time-dependent DFT, UV/Vis spectral predictions were calculated via the more recently introduced domain-based local pair natural orbital similarity transformed equation of motion-coupled cluster singles and doubles (STEOM-DLPNO-CCSD)[31] using keywords `STEOM-DLPNO-CCSD DEF2-TZVP DEF2-TZVP/C RijCosX CPCM(Benzene)`. Due to the computationally expensive nature of this method, ethyl and dipp groups on the ligand were reduced in size to methyl as displayed below. Calculations were carried out on a personal workstation via the use of a 1 TB NVMe SSD as virtual memory. Data was convoluted with a gaussian of peak width 15 nm and visualized in Avogadro. The results indicated that the [2.2.2] bicyclic phosphaborene that would result from phosphinidine insertion into a ring B-C bond is likely sensitive to light of the same wavelength required for decarbonylation, thus its isolation (if formed) would be difficult.

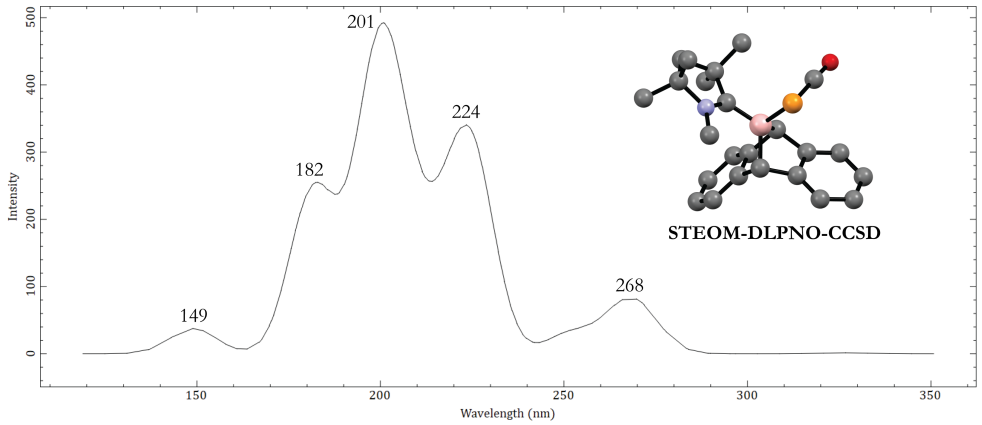

Figure 3-14: Predicted UV/Vis absorption spectrum of CAAC·ABPCO carried out using the STEOM-DLPNO-CCSD method.

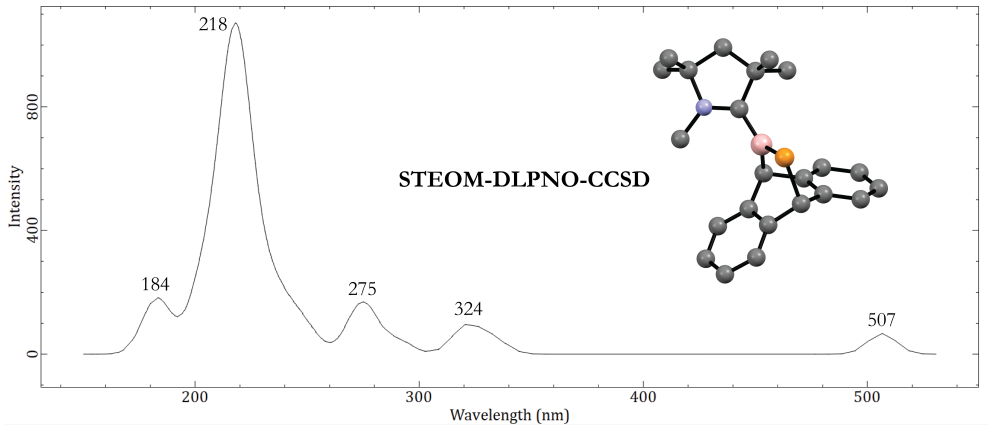

Figure 3-15: Predicted UV/Vis absorption spectrum of hypothetical CAAC·BPA carried out using the STEOM-DLPNO-CCSD method.

Bibliography

[1] Paetzold, P. *Advances in Inorganic Chemistry*; Elsevier, 1987; Vol. 31; pp 123–170.

[2] Bartlett, R. A.; Feng, X.; Power, P. P. Synthesis and characterization of the phosphinidene borate complexes [Li(Et2O)2PRB(Mes)2] and [Li(12-crown-4)2][RPB(Mes)2].cntdot.THF [R = Ph, C6H11 or Mes (Mes = 2,4,6-Me3C6H2)]: the first structurally characterized boron-phosphorus double bonds. *Journal of the American Chemical Society* **1986**, *108*, 6817–6819.

[3] Price, A. N.; Nichol, G. S.; Cowley, M. J. Phosphaborenes: Accessible Reagents for the Synthesis of CC/PB Isosteres. *Angewandte Chemie International Edition* **2017**, *56*, 9953–9957.

[4] Linti, G.; Nöth, H.; Polborn, K.; Paine, R. T. An Allene-analogous Boranylidenephosphane with BP Double Bond: 1,1-Diethylpropyl(2,2,6,6-tetramethylpiperidino)-boranylidenephosphane-P-pentacarbonylchromium. *Angewandte Chemie International Edition in English* **1990**, *29*, 682–684.

[5] Knabel, K.; Klapötke, T. M.; Nöth, H.; Paine, R. T.; Schwab, I. A Bicyclic P–P-Bridged 1,3,2,4-Diphosphadiboretane Cation and an Imino(phosphinidene)borane–$AlBr_3$ Adduct. *European Journal of Inorganic Chemistry* **2005**, *2005*, 1099–1108.

[6] Rivard, E.; Merrill, W. A.; Fettinger, J. C.; Power, P. P. A donor-stabilization strategy for the preparation of compounds featuring PB and AsB double bonds. *Chem. Commun.* **2006**, 3800–3802.

[7] Rivard, E.; Merrill, W. A.; Fettinger, J. C.; Wolf, R.; Spikes, G. H.; Power, P. P. BoronPnictogen Multiple Bonds: Donor-Stabilized PB and AsB Bonds and a Hindered Iminoborane with a BN Triple Bond. *Inorganic Chemistry* **2007**, *46*, 2971–2978.

[8] Koner, A.; Morgenstern, B.; Andrada, D. M. Metathesis Reactions of a NHC-Stabilized Phosphaborene. *Angewandte Chemie International Edition* **2022**, *61*.

[9] Yang, W.; Krantz, K. E.; Dickie, D. A.; Molino, A.; Wilson, D. J. D.; Gilliard, R. J. Crystalline BP-Doped Phenanthryne via Photolysis of The Elusive Boraphosphaketene. *Angewandte Chemie International Edition* **2020**, *59*, 3971–3975.

[10] Li, J.; Lu, Z.; Liu, L. L. A Free Phosphaborene Stable at Room Temperature. *Journal of the American Chemical Society* **2022**, *144*, 23691–23697.

[11] LaPierre, E. A.; Patrick, B. O.; Manners, I. A Crystalline Monomeric Phosphaborene. *Journal of the American Chemical Society* **2023**, *145*, 7107–7112.

[12] Pyykkö, P. Additive Covalent Radii for Single-, Double-, and Triple-Bonded Molecules and Tetrahedrally Bonded Crystals: A Summary. *The Journal of Physical Chemistry A* **2015**, *119*, 2326–2337.

[13] Hagspiel, S.; Fantuzzi, F.; Dewhurst, R. D.; Gärtner, A.; Lindl, F.; Lamprecht, A.; Braunschweig, H. Adducts of the Parent Boraphosphaketene H $_2$ BPCO and their Decarbonylative Insertion Chemistry. *Angewandte Chemie International Edition* **2021**, *60*, 13666–13670.

[14] Wilson, D. W. N.; Franco, M. P.; Myers, W. K.; McGrady, J. E.; Goicoechea, J. M. Base induced isomerisation of a phosphaethynolato-borane: mechanistic insights into boryl migration and decarbonylation to afford a triplet phosphinidene. *Chemical Science* **2020**, *11*, 862–869.

[15] Swarnakar, A. K.; Hering-Junghans, C.; Nagata, K.; Ferguson, M. J.; McDonald, R.; Tokitoh, N.; Rivard, E. Encapsulating Inorganic Acetylene, HBNH, Using Flanking Coordinative Interactions. *Angewandte Chemie International Edition* **2015**, *54*, 10666–10669.

[16] Braunschweig, H.; Kupfer, T.; Radacki, K.; Schneider, A.; Seeler, F.; Uttinger, K.; Wu, H. Synthesis and Reactivity Studies of Iminoboryl Complexes. *Journal of the American Chemical Society* **2008**, *130*, 7974–7983.

[17] Cory, D.; Ritchey, W. Suppression of signals from the probe in bloch decay spectra. *Journal of Magnetic Resonance (1969)* **1988**, *80*, 128–132.

[18] Drance, M. J.; Sears, J. D.; Mrse, A. M.; Moore, C. E.; Rheingold, A. L.; Neidig, M. L.; Figueroa, J. S. Terminal coordination of diatomic boron monofluoride to iron. *Science* **2019**, *363*, 1203–1205.

[19] Braunschweig, H.; Radacki, K.; Schneider, A. Oxoboryl Complexes: Boron Oxygen Triple Bonds Stabilized in the Coordination Sphere of Platinum. *Science* **2010**, *328*, 345–347.

[20] Pangborn, A. B.; Giardello, M. A.; Grubbs, R. H.; Rosen, R. K.; Timmers, F. J. Safe and Convenient Procedure for Solvent Purification. *Organometallics* **1996**, *15*, 1518–1520.

[21] Williams, D. B. G.; Lawton, M. Drying of Organic Solvents: Quantitative Evaluation of the Efficiency of Several Desiccants. *The Journal of Organic Chemistry* **2010**, *75*, 8351–8354.

[22] Lenz, P.; Oshimizu, R.; Klabunde, S.; Daniliuc, C. G.; Mück-Lichtenfeld, C.; Tendyck, J. C.; Mori, T.; Uhl, W.; Hansen, M. R.; Eckert, H.; Yamaguchi, S.; Studer, A. Oxy-Borylenes as Photoreductants: Synthesis and Application in Dehalogenation and Detosylation Reactions. *Angewandte Chemie International Edition* **2022**, *61*.

[23] Puschmann, F. F.; Stein, D.; Heift, D.; Hendriksen, C.; Gal, Z. A.; Grützmacher, H.-F.; Grützmacher, H. Phosphination of Carbon Monoxide: A Simple Synthesis of Sodium Phosphaethynolate (NaOCP). *Angewandte Chemie International Edition* **2011**, *50*, 8420–8423.

[24] Plotkin, J. S.; Shore, S. G. Convenient preparation and isolation of pure potassium cyclopentadienyldicarbonylferrate, K[(.eta.5-C5H5)Fe(CO)2]. *Inorganic Chemistry* **1981**, *20*, 284–285.

[25] Fischer, M.; Schmidtmann, M. B(C $_6$ F $_5$) $_3$ - and HB(C $_6$ F $_5$) $_2$ -mediated transformations of isothiocyanates. *Chemical Communications* **2020**, *56*, 6205–6208.

[26] Fulmer, G. R.; Miller, A. J. M.; Sherden, N. H.; Gottlieb, H. E.; Nudelman, A.; Stoltz, B. M.; Bercaw, J. E.; Goldberg, K. I. NMR Chemical Shifts of Trace Impurities: Common Laboratory Solvents, Organics, and Gases in Deuterated Solvents Relevant to the Organometallic Chemist. *Organometallics* **2010**, *29*, 2176–2179.

[27] Sheldrick, G. M. SHELXT – Integrated space-group and crystal-structure determination. *Acta Crystallographica Section A Foundations and Advances* **2015**, *71*, 3–8.

[28] Müller, P.; Herbst-Irmer, R.; Spek, A. L.; Schneider, T. R.; Sawaya, M. R. *Crystal Structure Refinement*; Oxford University Press, 2006.

[29] Müller, P. Practical suggestions for better crystal structures. *Crystallography Reviews* **2009**, *15*, 57–83.

[30] Neese, F. Software update: The ORCA program system—Version 5.0. *WIREs Computational Molecular Science* **2022**, *12*.

[31] Berraud-Pache, R.; Neese, F.; Bistoni, G.; Izsák, R. Unveiling the Photophysical Properties of Boron-dipyrromethene Dyes Using a New Accurate Excited State Coupled Cluster Method. *Journal of Chemical Theory and Computation* **2020**, *16*, 564–575.